



City Research Online

City St George's, University of London

Citation: Alam, N., Maraveas, C., Tsavdaridis, K. D. & Nadjai, A. (2021). Performance of Ultra Shallow Floor Beams (USFB) exposed to standard and natural fires. *Journal of Building Engineering*, 38, 102192. doi: 10.1016/j.jobe.2021.102192

This is the accepted version of the paper.

This version of the publication may differ from the final published version. To cite this item please consult the publisher's version.

Permanent repository link: <https://openaccess.city.ac.uk/id/eprint/27685/>

Link to published version: <https://doi.org/10.1016/j.jobe.2021.102192>

Copyright and Reuse: Copyright and Moral Rights remain with the author(s) and/or copyright holders. Copies of full items can be used for personal research or study, educational, or not-for-profit purposes without prior permission or charge, unless otherwise indicated, provided that the authors, title and full bibliographic details are credited, a hyperlink and/or URL is given for the original metadata page and the content is not changed in any way. For full details of reuse please refer to [City Research Online policy](#).

1 Performance of Ultra Shallow Floor Beams (USFB) exposed to 2 standard and natural fires

3
4 Naveed Alam¹, Chrysanthos Maraveas², Konstantinos Daniel Tsavdaridis³, Ali Nadjai¹

5
6 ¹FireSERT, School of Built Environment, Ulster University, Belfast, UK

7 ²Department of Civil Engineering, University of Patras, Patra, Greece

8 ³School of Civil Engineering, University of Leeds, Leeds, UK

9
10 Corresponding author: C. Maraveas: c.maraveas@maraveas.gr

11 **Abstract**

12
13
14 This paper investigates computationally the fire performance of a plug steel-concrete composite
15 flooring system, the partially encased ultra-shallow floor beams (USFB). The investigation of the
16 behaviour of USFBs exposed to standard and natural fires is crucial in determining their fire
17 resistance and evaluating their overall performance in contemporary construction. Although the
18 product providers usually indicate the fire resistance of USFBs based on EN1994-1-2
19 procedures, the response to elevated temperature effects remains yet neither well documented
20 nor clearly understood. This analysis involves two different beams of 5m and 8m span. Results
21 show that the unprotected beams experience severe temperature gradients while exposed to
22 standard fire, as the lower flange still remains unprotected in contrast to the upper steel parts of
23 the cross-section which are encased in concrete. Their fire resistance rating is found
24 approximately at 40 mins. Moreover, different thermal gradients are developed when the USFBs
25 are exposed to natural fires (slow and fast burning). When the lower flange is protected with
26 intumescent coatings, the USFBs have shown increased fire resistance and they can survive a
27 full duration of a natural fire under realistic utilization ratios. From the parametric analyses, the
28 optimized thicknesses for the required intumescent coating were obtained to achieve 60, 90,
29 and 120 min of fire resistance and for surviving of natural fires exposures.

30
31 **Keywords:** Ultra Shallow Floor Beams; Flooring systems; Fire resistance; Intumescent
32 coating; Fire; Standard Fire; Natural Fires

33

34 **Introduction**

35 The design of composite steel-concrete beams has evolved over the years and significant
36 improvements have been seen in the last three decades. One of these innovative designs is the
37 Ultra-shallow floor beam (USFB) with plug composite system. These beams were developed
38 and introduced in UK in 2006 by Westok Ltd. (UK). USFBs are formed by welding two highly
39 asymmetric steel Tees, cut from a universal beam section and a universal column section, along
40 their web. The lower Tee is usually larger as compared to the upper Tee. USFBs can be used
41 with pre-cast concrete slabs as well as with deep steel decking; the latter offers a decreased
42 self-weight and thus is more popular [1]. The steel web of these beams has continuous
43 periodical web openings along the length, alike cellular beams, as a result concrete passes
44 through these openings during casting and provides connectivity to the concrete slab on both
45 sides. This concrete between the flanges and in the openings can enhance the longitudinal and
46 vertical shear strength of the USFBs [2].

47 When comparing USFBs with normal composite steel-concrete beams (down-stand beams),
48 USFBs are far shallower systems thus reducing the structural depth significantly. The shear
49 connection is very strong in comparison to standard headed shear studs on the top of the steel
50 flange in down-stand beams, due to the concrete which is passing through some web openings
51 and it provides continuity to the slab, with the use of either tie-bars, horizontally web-welded
52 shear studs, or ducting. Full service integration can be achieved when deep profiled steel
53 decking is employed, as pipes or ducts pass through the beam, between the ribs of the steel
54 decking, and typically every few web openings which are not filled by concrete. In the case of
55 precast units, all web openings are filled by in-situ concrete to provide the cohesion between the
56 precast units and the steel beam, hence service integration is not provided. This concrete plug
57 system forms a unique mechanism for transferring longitudinal shear forces along the beam.
58 Moreover, the asymmetric perforated steel beam does not buckle as the beam is partially
59 encased by the concrete, which also provides added fire resistance to the steel as opposed to
60 down-stand beams. Furthermore, USFBs minimise the need for propping during construction.
61 Extensive research has been conducted to study the response of USFBs at ambient
62 temperatures via experimental investigations and finite element modelling (FEM). These studies
63 include investigations on their horizontal shear resistance [3], their vertical shear resistance [4]

64 as well as their vibration performance [5] at ambient temperatures. Although experimental and
65 analytical investigations are available related to the performance of USFBs at ambient
66 temperatures [2,4], the studies addressing their performance at elevated temperatures are
67 limited to a study related to the unprotected USFBs exposed to standard fire [6]. Despite the
68 unavailability of satisfactory studies related to their fire performance, the manufacturing
69 companies certify their fire resistance and insulation requirements based on the Eurocode
70 procedures, EN 1994-1-2 (2014)[7].

71 Having recognised the existing knowledge gaps with regards to the applicability of the
72 Eurocodes related to their fire performance, a detailed investigation was conducted herein to
73 understand the performance of unprotected as well as protected USFBs exposed to standard
74 and natural fires. Previous studies have shown that natural fires result in different temperature
75 distributions and thermal gradients and significantly affect the performance of partially protected
76 steel beams [8,9]. FEM was conducted using the commercial programme ABAQUS version
77 2019. The methodology used in this research follows the same principles and procedures used
78 to successfully simulate the performance of asymmetric slim floors in fire against fire test results
79 as presented by Alam et al, 2018 [8] and Maraveas et al, 2012 [10].

80 To study the performance of protected and unprotected USFBs, FEM was performed for two
81 simply supported specimens; a 5 m span and a 8 m span. Further details related to sizes,
82 shapes and arrangements are available in Maraveas et al, 2015 [6]. A summary of these details
83 is reproduced in section 2 for the ease of the reader.

84 The basic findings of the research are that USFBs can survive of a parametric fire with minimum
85 of protection. On the contrary, to archive high fire resistance when exposed to standard fires,
86 USFBs require thick layer of intumescent coating or a combination of low load ratio and
87 protection with intumescent coating.

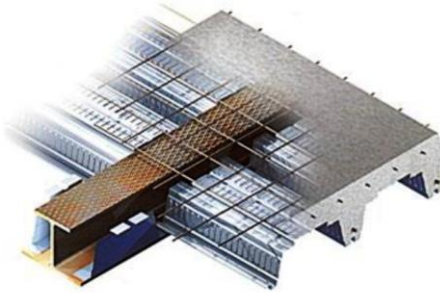
88

89 **1. USFB SYSTEM DETAILS**

90 As Ultra-Shallow Floor Beams (USFB) connect with the floor slab on both sides of the
91 steel web via the concrete passing through the web opening [4] (Figure 1). Such slim-floor type
92 composite systems also have other advantages, including increased load carrying capacity, fire
93 resistance, local buckling stiffness and a significant increase in the bending stiffness due to the

94 plug mechanism when compared with traditional steel-concrete composite beams. The plug
95 composite actions is achieved through various ways most commonly by providing steel
96 reinforcement through the web openings perpendicular to the steel beam section as shown in
97 Figure 1 (c). In other words, the reinforcement is transverse to the web of the beam and is
98 passing via the web openings to develop the continuity from one side to the other, and thus
99 increase the longitudinal shear (See Figure 1c). This is called a plug system. In addition, these
100 structures reduce construction cost by eliminating the construction time and reducing the
101 requirements of formwork – no need for slab propping [2,11].The most common applications of
102 USFBs have been with slabs having depths ranging from 180mm to 300mm, in which the
103 concrete has been placed level with the top flange. The practical span to depth ratio of USFBs
104 is usually in the range of 25 to 30. Consequently, the USFB is limited to a span up to 9m, with a
105 depth of up to 300mm. When the span is extended to more than 9m, the depth will increase to
106 more than 300mm, even when lightweight concrete is used [2,11]. This results to an
107 uneconomical solution for flooring systems. Moreover, an increase of slab spans reduces the
108 natural frequencies of the USFBs, leading to an increase of the floor vibration [5].

109 (a)



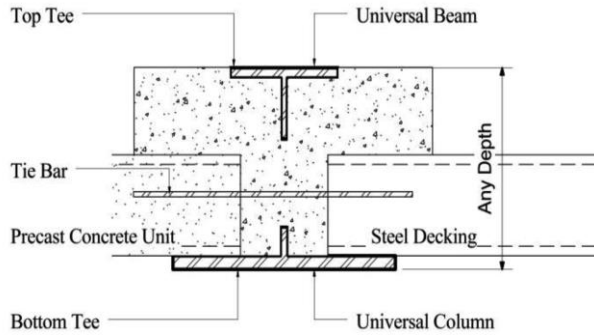
110
111

(b)



112
113

(c)

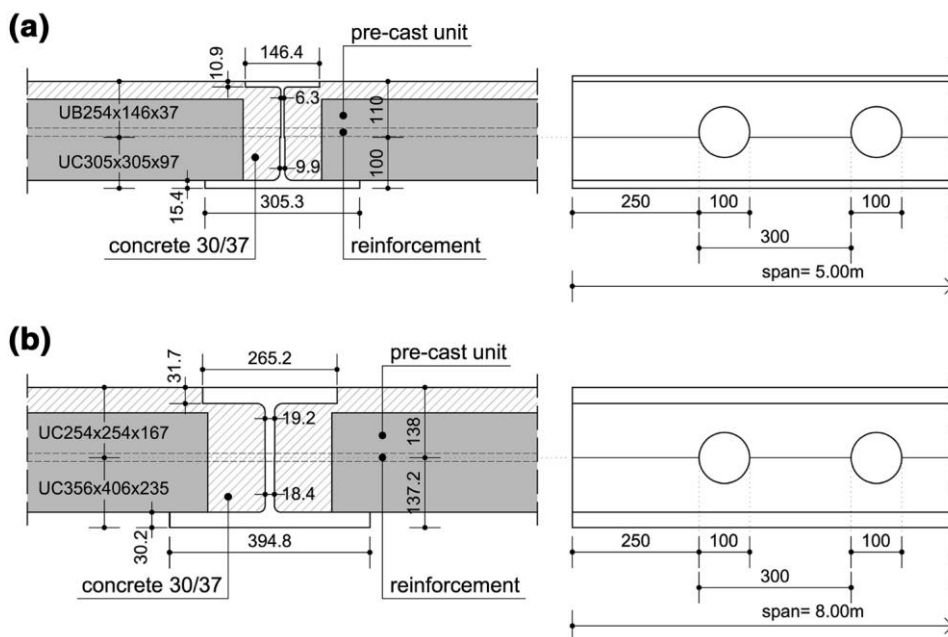


114
115
116
117
118

Figure 1. (a), (b) construction arrangements of USFBs [1] and (c) typical cross-section of USFBs [5]

119 **2. SIMULATED USFB SYSTEMS**

120 During this investigation, two typical USFBs have been analysed. Both beams are considered
121 as simply supported. USFB-1 has a 5 m span and has a total section depth of 220 mm. The top
122 Tee of the USFB section is cut from a 254 x 146 x 37 UB section while the bottom Tee has been
123 taken from 254 x 254 x 167 UC section as shown in Figure 2(a). USFB-2 had an 8 m span and
124 consisted of a 254 x 254 x 167 UC top Tee and a 356 x 406 x 235 UC bottom Tee (Figure 2b).
125 Additionally, two steel reinforcing bars were applied to the tension zone of USFB-2 to replicate
126 the construction practices. In both cases, the effective width of the USFB assemblies has been
127 taken equal to $L/8$ for analytical modelling purposes. The maximum load capacities for these
128 specimens were calculated and presented earlier by Maraveas et al (2015)[6] which have been
129 adopted during this study.



130

131 **Figure 2.** Details of the USFBs used for numerical simulation (a) Beam A and (b) Beam B [6].
132

133 **3 Numerical Modelling**

134 **3.1 Material Properties**

135 The material properties for structural steel, steel reinforcement and the concrete are adopted
136 following the recommendations of the Eurocodes, EN 1994-1-2 (2014) [7]. The material stress-
137 strain relationships at room temperature are based on the design values defined in Eurocodes.
138 The material safety factor considered according to UK National Annex for fire design ($\gamma_M=1,00$)
139 for structural steel, steel reinforcement and concrete. The structural steel was modelled using a
140 yield strength of 355 MPa while the concrete was modelled with a compression strength of 35
141 MPa. Further, the tensile strength of the concrete was also considered following the
142 recommendations of the Eurocodes, EN 1994-1-2 (2014) [7]. The density of concrete was
143 taken 2400 kg/m³ for concrete while the same was taken 7850 kg/m³ for the structural and
144 reinforcing steel. The thermal properties (thermal conductivity and specific heat), the mechanical
145 properties and thermal expansion of steel and concrete are taken from EN 1994-1-2 (2014) [7].
146

147 **3.2 Modelling of intumescent coatings**

148 The fire protection material used during this investigation is in the form of intumescent coatings.
149 The behaviour of intumescent coatings in fire has been of great interest amongst the
150 researchers in the recent past and numerous publications are available. The majority of the
151 literature focuses on their behaviour under cone calorimeters or in standard fire exposure
152 conditions similar to the work conducted by de Silva et al (2019) [12]. The section factors used
153 during these investigations are also limited. A detailed literature review on the performance of
154 intumescent coatings exposed to different scenarios suggests that one of the most
155 comprehensive experimental studies in this regard was conducted by Cirpici et al (2016) [13]. In
156 additional to the standard fire, two natural fire scenarios, a fast fire and a slow fire, were also
157 considered during the investigation. During the research conducted by Cirpici et al (2016) [13],
158 various investigations were carried out to analyse the behaviour of intumescent coatings applied
159 to steel specimens with different section factors. These section factors were 333 m⁻¹, 200 m⁻¹,
160 100 m⁻¹ and 50 m⁻¹. In addition, the effectiveness of the thicknesses of intumescent coatings

161 was investigated considering specimens with thickness of intumescent coatings equal to either
162 0.4 mm, 0.8 mm, 1.2 mm, 1.6 mm, or 2.0 mm.

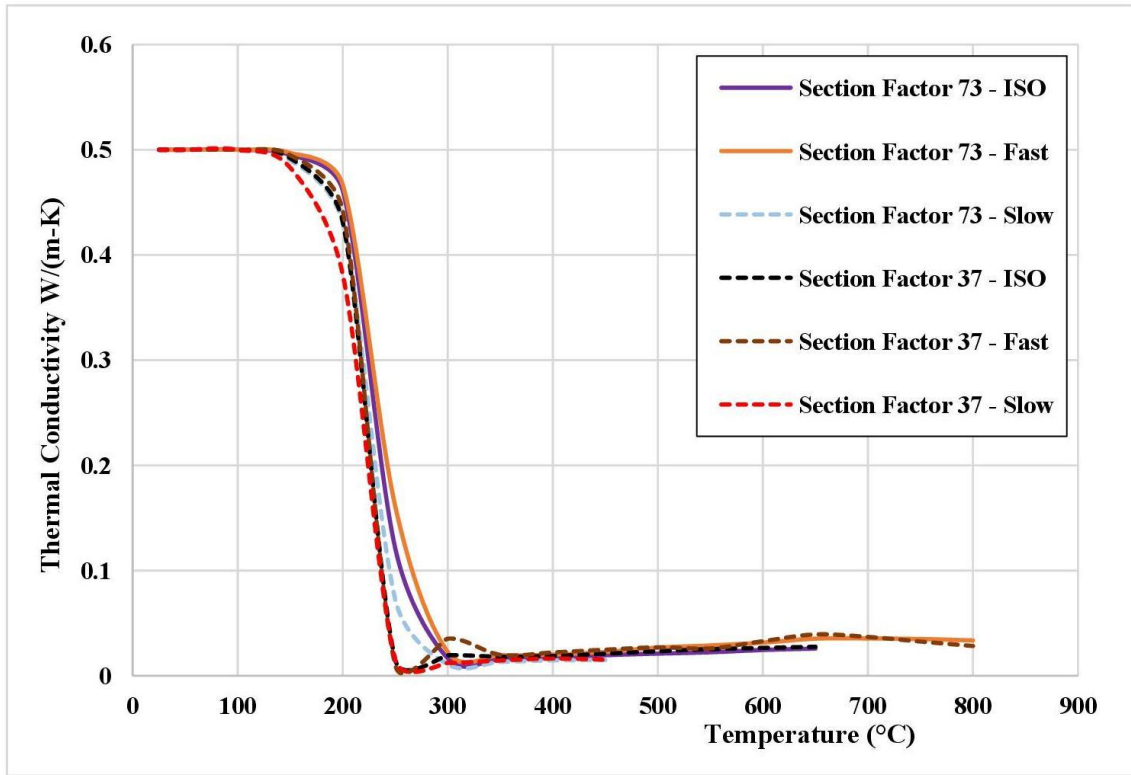
163 During this study, the specific heat of the intumescent coatings is taken as 1000 J/kg K and the
164 density is 1300 kg/m³ as proposed by Dai et al (2010) [14]. It is considered that the quantity of
165 intumescent coatings is significantly smaller as compared to the structural elements, i.e., the
166 influence of density and specific heat is insignificant considering the heat transfer through
167 intumescent coatings being predominantly via conduction [12]. The thermal conductivity of
168 intumescent coating is taken considering its dependency on fire exposure conditions (heating
169 rate), the section factors as well as its thickness. During this investigation, three fire exposure
170 scenarios are considered, the standard fire, the fast-natural fire, and the slow natural fire. Three
171 different thicknesses of the intumescent coatings are considered, 1.2 mm, 0.8 mm and 0.4 mm.
172 It was found that the section factors for USFB-1 (Figure 2(a)) and USFB-2 (Figure 2(b)) were 73
173 m⁻¹ and 37 m⁻¹, respectively. To obtain the temperature dependent thermal conductivity for
174 these section factors, linear interpolation and extrapolation was conducted using the values
175 reported for section factors 100 m⁻¹ and 50 m⁻¹ by Cirpici et al (2016)[13]. The values of
176 temperature dependent thermal conductivity of intumescent coating for section factors 73 m⁻¹
177 and 37 m⁻¹ under different fire exposure conditions are presented in Figure 3 for thickness 1.2
178 mm, 0.8 mm, and 0.4 mm, respectively. These values have been used for the analytical
179 modelling of thermal performance of intumescent coatings during this investigation.

180 The contribution of intumescent coatings towards the mechanical response of the protected
181 USFBs is considered negligible. Hence, no mechanical properties have been used during the
182 analytical modelling.

183

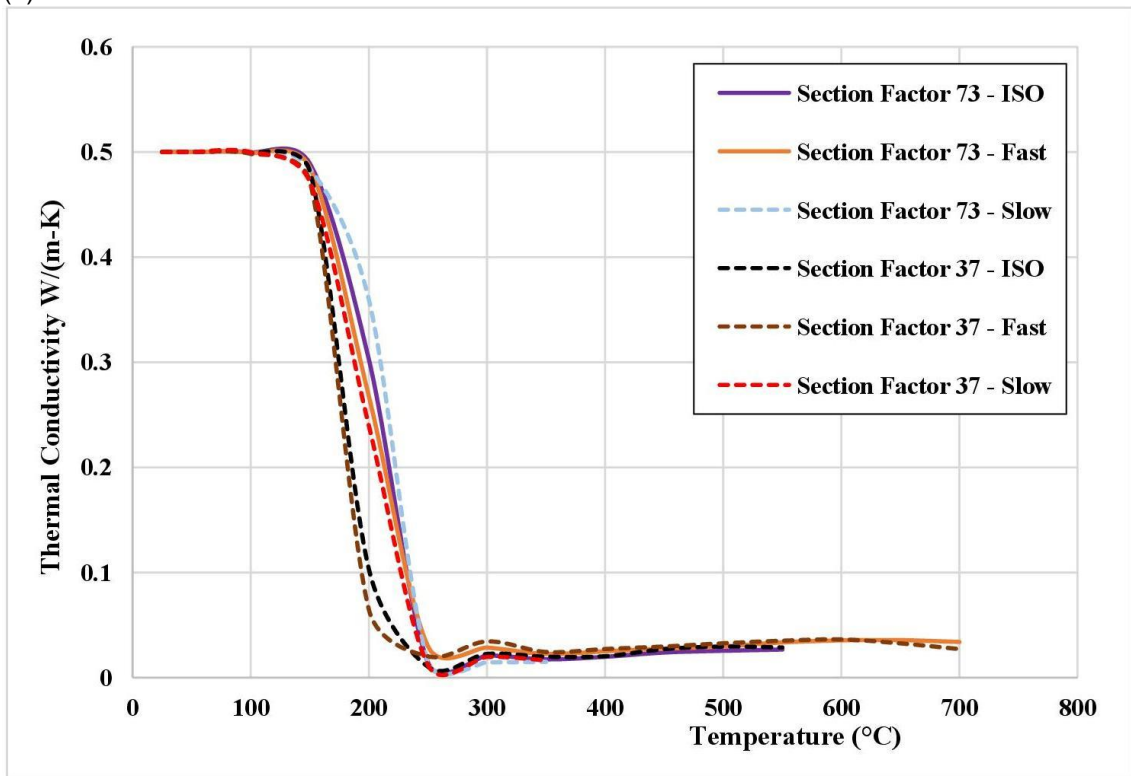
184

185 (a)



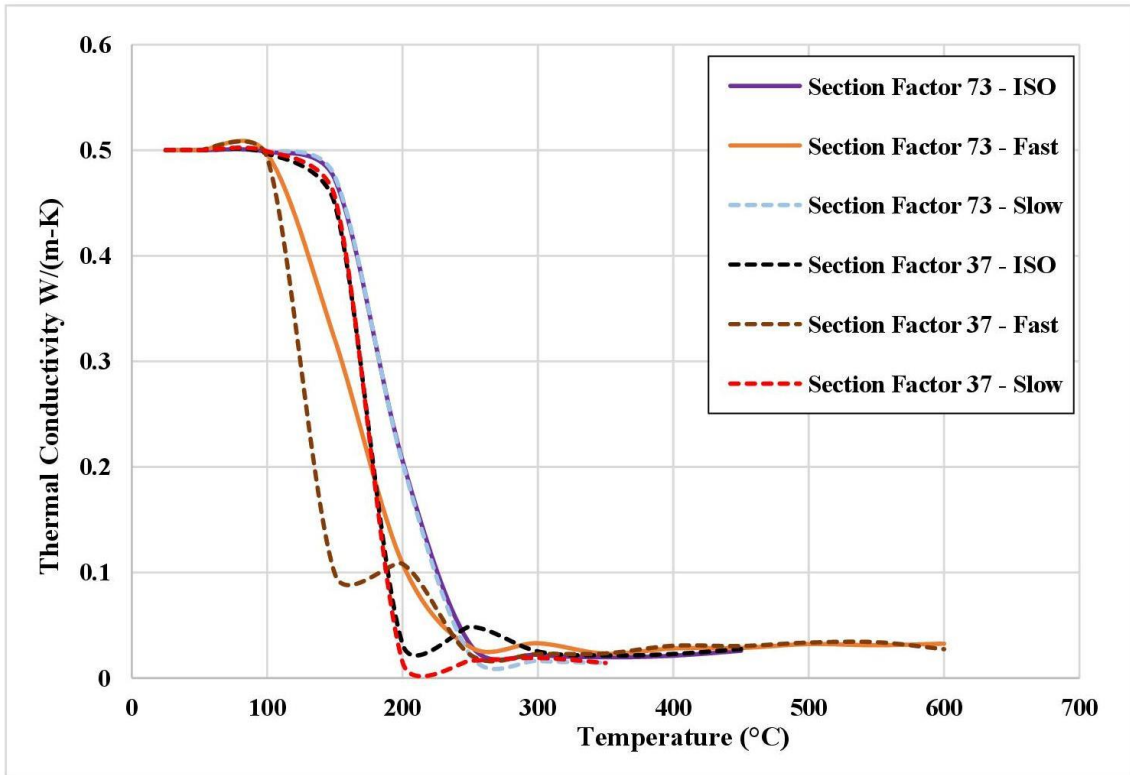
186
187

(b)



188
189

(c)



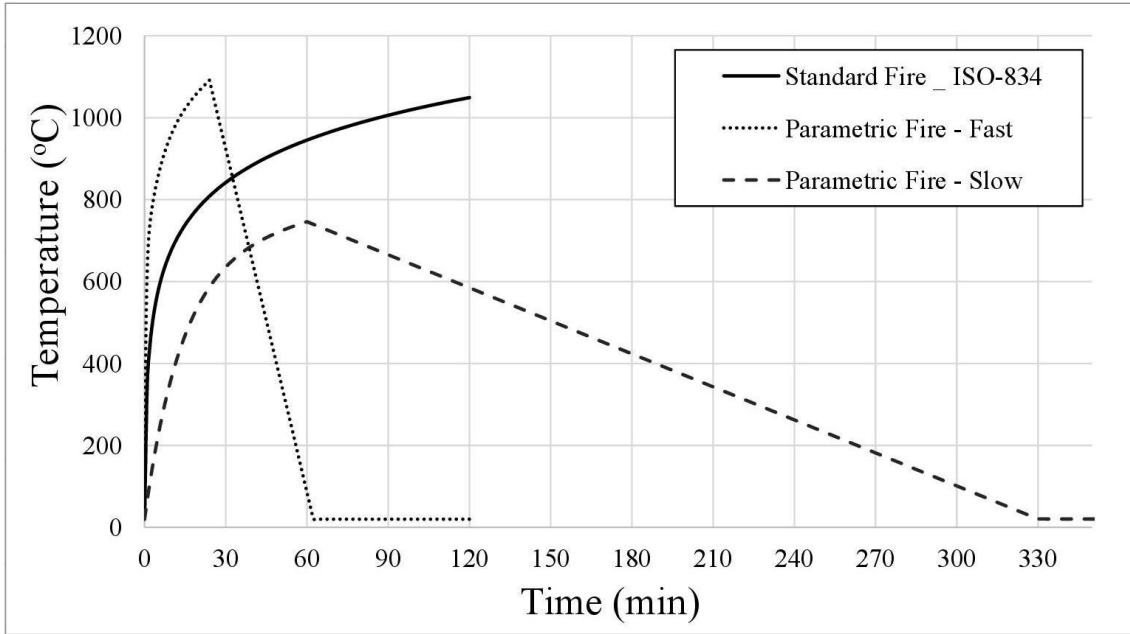
190
191
192
193
194
195
196
197

Figure 3. Temperature dependent thermal conductivity for intumescent coating with (a) 1.2 mm thickness under different fire exposure conditions for section factors 73m^{-1} and 37m^{-1} , (b) 0.8 mm thickness under different fire exposure conditions for section factors 73m^{-1} and 37m^{-1} and (c) 0.4 mm thickness under different fire exposure conditions for section factors 73m^{-1} and 37m^{-1}

3.3 The fire exposure conditions

198 Eurocodes provide different fire exposure scenarios in terms of standard fire models as well as
199 the natural fire models in section 3.2 and 3.3 of EN 1991-1-2 (2009)[15]. The fire exposure
200 scenarios used during this research are presented in Figure 4.

201
202 The natural fire curves shown in Figure 4 have been produced according EN 1991-1-2 (2009)
203 [15]. For this purpose, the fire compartment has been assumed to be a representative of an
204 office building with a fire load density ($q_{i,d}$) equal to 200 MJ/m^2 . The representation of
205 compartment boundaries in terms of density, specific heat and thermal conductivity are taken in
206 terms of 'b' as defined in EN 1991-1-2 (2009)[15]. The value of 'b' is equal to $1120\text{ J/M}^2\text{s}^{1/2}\text{K}$
207 both for the fast and the slow natural fire. The value of opening factor for the fast fire is taken
208 equal to $0.1\text{ m}^{1/2}$ while the one for the slow fire is taken as $0.02\text{ m}^{1/2}$ - the minimum value
209 proposed by EN 1991-1-2. These parametric fires cover a wide range of natural (compartment)
210 fires enabling its general applicability. A similar approach is previously used by Alam et al
211 (2018) [16] to study the response of slim floors beams at elevated temperatures.



212
213
214
215

Figure 4. Considered standard and natural fire curves

216 **3.4 Numerical Modelling**

217 **3.4.1 Unprotected USFBs**

218 Finite element modelling for the unprotected USFBs is performed using the two-phase method
 219 explained and presented by Maraveas et al (2015) [6]. In the initial phase, temperature contours
 220 for the USFBs are obtained by performing the thermal analysis. The convection coefficients for
 221 exposed and unexposed surfaces are taken equal to 25 W/m²K and 9 W/m²K, respectively. The
 222 radiation emissivity for the bottom steel flange and the composite floor is taken as 0.7 following
 223 the EN1994-1-2 (2014) [7] recommendations. Both concrete and steel are modelled using the 8-
 224 node linear brick elements, DC3D8 and the interface between the steel and the concrete is
 225 modelled as a perfect thermal contact allowing full heat transfer. For each unprotected USFB,
 226 three thermal analyses are performed - the standard fire exposure conditions, the fast natural
 227 fire and the slow natural fire. Details related to the fire exposure conditions are provided earlier
 228 in section 3.3.

229 The second phase of the numerical modelling consists of the thermo-mechanical analysis and is
 230 performed in two steps. During the first step, external loads representing the degree of
 231 utilization of USFBs are applied while in the second step, the USFB specimens are heated
 232 using the thermal contours obtained during the first phase. The external loads applied were

233 uniformly distributed along the length of each beam. The concrete part is modelled using 8-node
234 linear brick elements (C3D8) considering the numerical instabilities associated with the inelastic
235 behaviour of concrete. On the other hand, the steel parts of the USFBs are modelled using
236 hexahedral elements with reduced integration (C3D8R). The analytical modelling was
237 conducted for USFBs under 55%, 70%, and 100% degrees of utilizations.

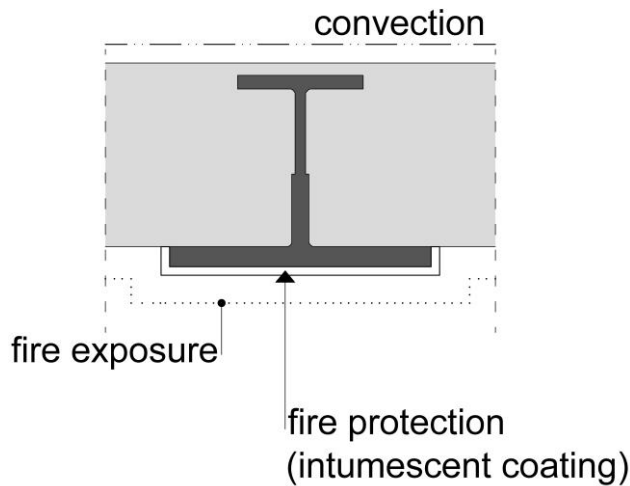
238

239 **3.4.2 Protected USFBs**

240 The protected USFB specimens were similar to the unprotected specimens with the exception
241 of a layer for intumescent coating modelled over the exposed bottom flange of the steel section.

242 The boundary conditions of the thermal analysis and the position of the insulation are shown in
243 Figure 5. Three FE models were prepared for each USFB. The first model consisted of an
244 intumescent layer of 1.2 mm on the exposed bottom flange while the second consisted of a 0.8
245 mm layer of protection. The last USFB model consisted of a 0.4 mm thick layer of intumescent
246 coating. The thermal analysis was performed using the 8-node linear brick elements, DC3D8 for
247 concrete, steel, and the intumescent coating. The convection coefficient and radiation emissivity
248 for exposed and unexposed surfaces of concrete and steel were same as that used for the
249 unprotected USFBs. However, the convection coefficient and radiation emissivity for the
250 intumescent coatings was taken as 20 W/m²K and 0.95, respectively as proposed by Bourbigot
251 et al (1995) [17]. A similar approach is also used by Alam et al (2018) [8] to study the
252 performance of protected slim floor beams exposed to elevated temperatures. The thermal
253 analysis for protected USFBs was performed for the three fire exposure scenarios discussed in
254 section 3.3.

255 During the thermo-mechanical analysis, no contribution of the intumescent coating was
256 considered as this material was only meant to protect against the elevated temperatures. The
257 thermo-mechanical analysis was the two-step method detailed earlier in section 3.4.1. Similar to
258 the unprotected case, the performance of USFBs was investigated for three degrees of
259 utilizations, 55%, 70%, and 100%.



260
261
262
263
264

Figure 5. Thermal analysis boundary conditions and the protected surface of the steel cross-section with intumescent coating.

265 **3.5 Validation of numerical models**

266 Fire tests on USFBs do not exist. For this reason, the validation performed against fire tests from
267 similar flooring systems. The methodology used during this research follows the same principles
268 and procedures used to successfully simulate the performance of asymmetric slim floors in fire
269 [10, 16] against fire test results. More specifically, two slim floor fire tests performed at
270 Warrington Fire Research Centre were successfully simulated with use of the described
271 methodology in previous sections in [10, 16]. Furthermore, validation of the used numerical
272 methodology for protected slim floors presented in section 3.2 is presented in [16].

273

274 **3.6 Load factor**

275 According to EN1994-1-2 (2009) [7], the design loads for the fire situation are given by the
276 equation:

277

$$278 \quad E_{fi,d} = n_{fi} E_d \quad (1)$$

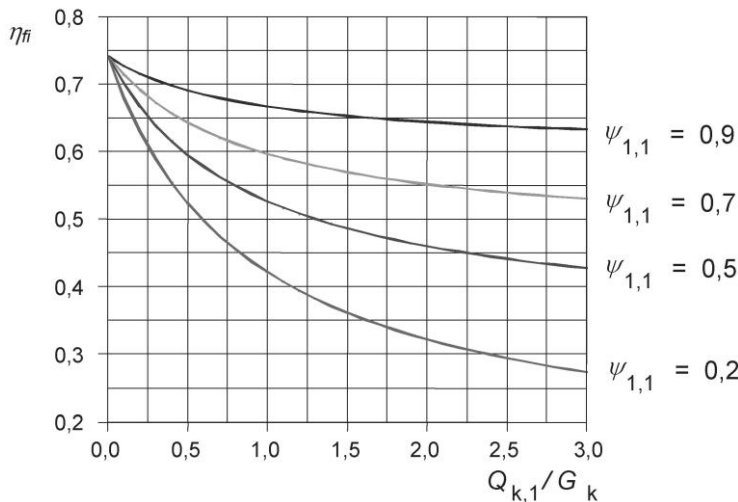
279

280 where E_d is the design value of the corresponding force for a fundamental combination of
281 actions, $E_{fi,d}$ is the design forces for fire design and n_{fi} is the reduction factor of E_d or called for
282 simplicity as load factor.

283 The load factor n_{fi} is a function of the reduction factor ψ_{fi} ($\psi_{1,1}$ or $\psi_{2,1}$) and of the ratio $Q_{k,1}/G_k$ and
 284 practically can take values between 0.75 and 0.25. EN1994-1-2 (2009) (Figure 6) suggests
 285 values of n_{fi} 0.65 or 0.70 (depending the use of the structure) for simplicity and without detailed
 286 calculation. This is a conservative assumption. Bailey (1999) [18] states that the loads expected
 287 in a fire event are in the range of 50 to 55% of the capacity of the structural members at ambient
 288 temperatures.

289 As the load factor cannot be determined, this research has a more general purpose, the
 290 analysis is performed for load factors 55%, 70%, and 100%. It must be noted that the load factor
 291 100% is not realistic and only included for comparison purposes. The ambient temperature
 292 loads are described in Maraveas et al (2015) [6]. The load applied as uniform load, before
 293 heating.

294 As the load factor is relevant to the applied design loads (E_d), the capacity of the structural
 295 element should be higher than E_d . In order to estimate the over-strength which may appear,
 296 information regarding the design per EN1994-1-1 (2004) [7] are presented in Table 1.



297

298 **Figure 6.** Reduction factor of the design value of the corresponding force for a fundamental
 299 combination of actions n_{fi} as a function of the ratio $Q_{k,1}/G_k$ and $\psi_{1,1}$ [7].
 300

301 **Table 1** Normal temperature maximum design unity factors for the critical load combination [6]
 302

Failure mode	Beam A	Beam B
Vertical shear	0.51	0.41

Horizontal shear	0.98	0.76
Moment shear interaction	1.00	0.91
Vierendeel bending	1.00	0.91
Longitudinal shear in slab	0.16	0.14
Vibration (Hz)	5.49	3.27
Imposed deflection (mm)	8.18	19.03

303

304 **4. FEM Results**

305 **4.1 Evaluation of numerical results**

306 The performance of USFB assemblies has been analysed following the deflection based failure
307 approach proposed in the British and International Standards. According to the British
308 Standards, BS 476 Part-20 (1999) [19] and ISO 834–1 (1987) [20], failure is deemed to occur
309 once the mid-span deflection of beams exceeds $L/20$ or the rate of deflection exceeds $L^2/9000d$,
310 L is the span while d is the overall depth of beam. The rate of deflection criteria is only
311 applicable once the mid-span deflection exceeds $L/30$ limits.

312

313 **4.2 Performance of unprotected USFBs**

314 In this section, the performance of unprotected USFBs is discussed in terms of developed
315 temperatures (thermal response) and fire resistance (structural response).

316

317 **4.2.1 Thermal response**

318 The temperature – time relationships for different fire exposures at different characteristic nodes
319 are presented in Figure 7. For both beams, the developed temperatures in nodes 3, 4, and 7 are
320 very low and, practically, the temperature does affect the mechanical properties of steel (<400
321 °C). As the shear connection between the steel beam and the concrete is undertaken due the

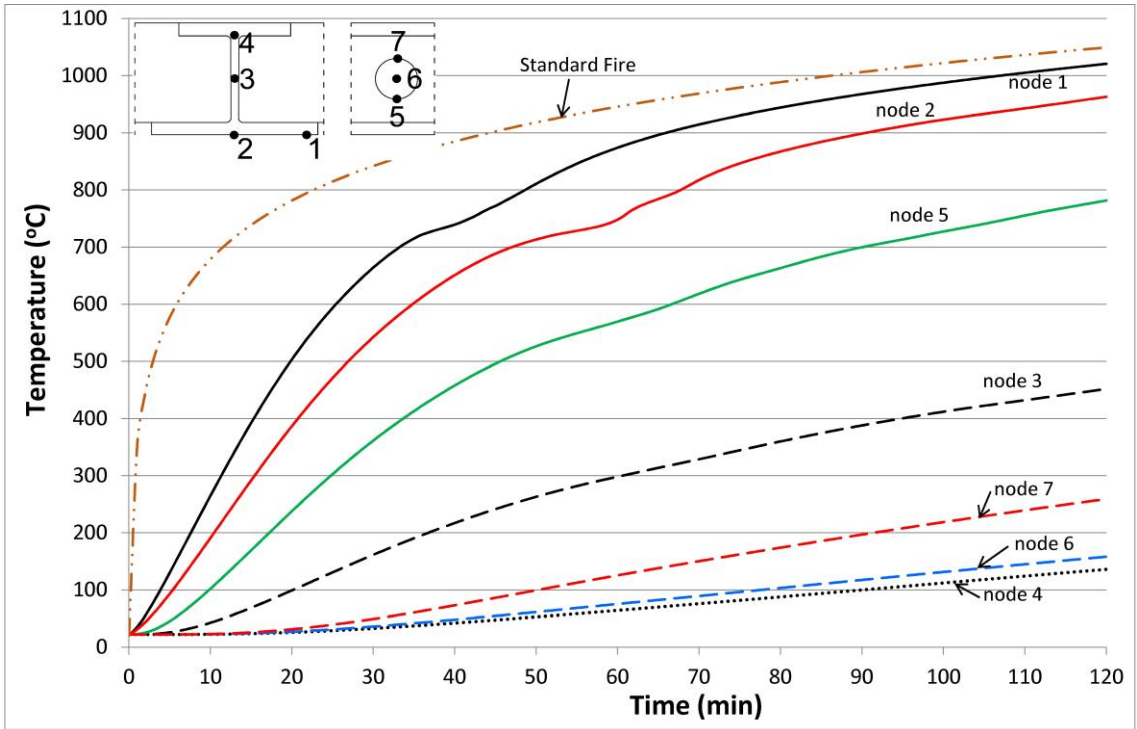
322 friction between the steel and concrete and via the concrete resistance and a tie bar in the web
323 opening while the developed temperatures are low, the shear connection is not affected by the
324 fire exposure. Similarly, approximately the 66% of the web develops temperatures lower than
325 400 °C, hence, the effect on its shear resistance is minimum.

326 As only the bottom flange is exposed to fire, it develops high temperatures (nodes 1 and 2,
327 Figure 7). The developed temperatures are higher in node 1 as it is near the corner of the
328 bottom flange – i.e., near the two exposed sides. Node 2 develops lower temperatures in
329 comparison to node 1, as the web absorbs the heat.

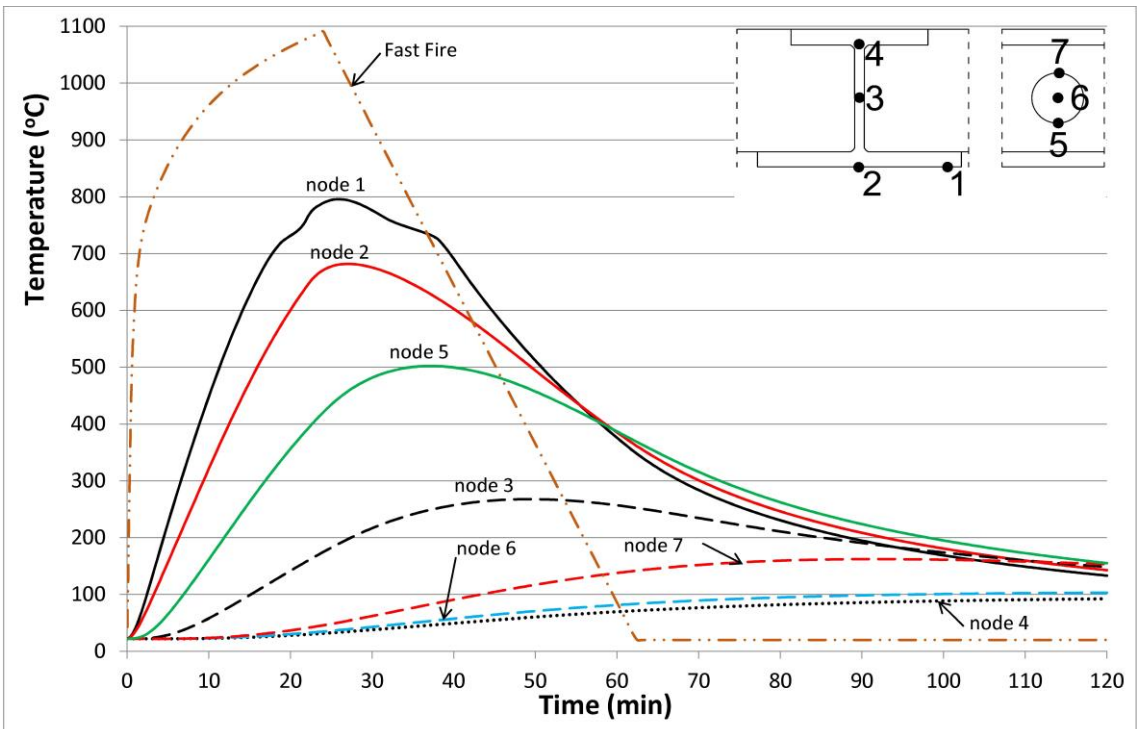
330 From the diagrams in Figure 7, it is clear that extreme thermal gradients are developed across
331 the USFBs. These thermal gradients depend on the fire exposure type. When the beam is
332 heated against the fast fire curve (Figure 4), due to the extremely rapid heating rate, the steel
333 cross-section develops extreme thermal gradients. When the beam is exposed to slow fire, the
334 heating is slow and for a longer duration, so the cross-section develops lower thermal gradients
335 and the developed temperatures are more uniform. When standard fire is used, the thermal
336 gradients are in between those obtained for fast and slow fires. For Beam A, the maximum
337 temperature is developed at node 1 for fast and slow fire exposures, the comparisons of
338 temperature profiles are presented in Tables 2 and 3, respectively. It must be noted that the
339 concrete slab develops higher thermal gradients than the steel section, given that the ratio of
340 the thermal conductivity of steel to the thermal conductivity of concrete is approximately five
341 times. The thermal gradients are increased, e.g., the non-uniform temperature distribution, when
342 the height of the cross-section is increased. Hence, Beam B (Figure 7(d), (e), (f)) with cross-
343 section height of 275.2 mm develops higher thermal gradients in comparison with Beam A
344 (Figure 7(a), (b), (c)) with cross-section height 200 mm.

345

346
347 (a)

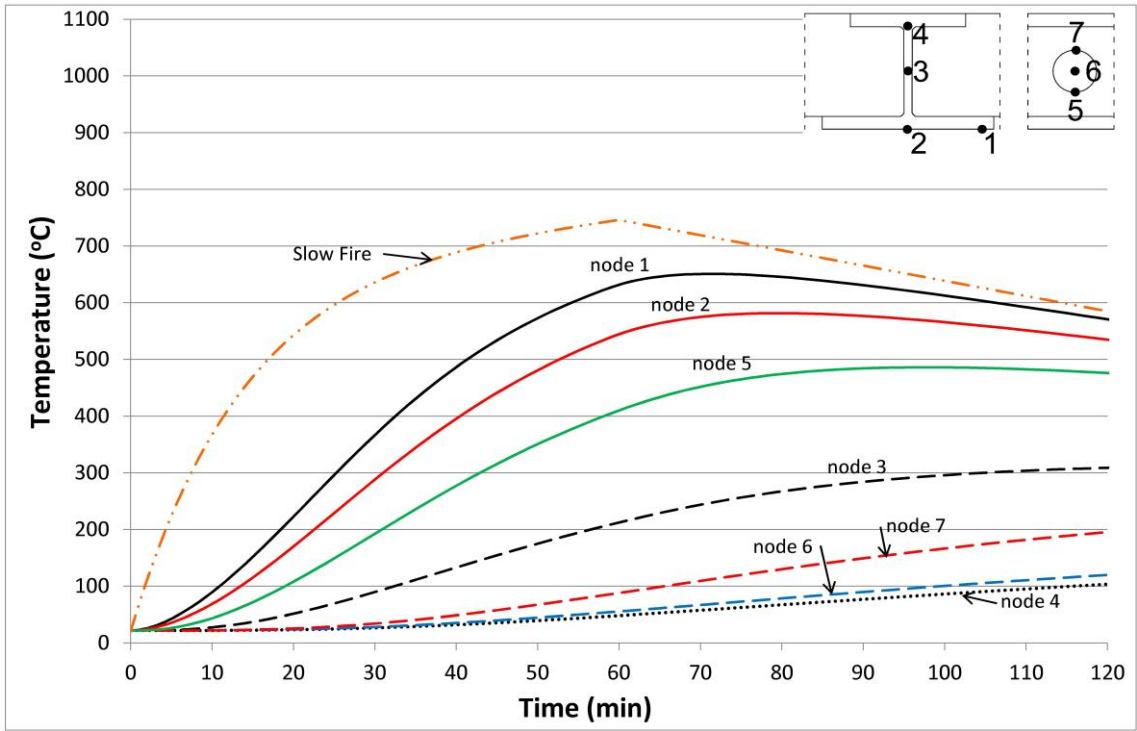


348
349 (b)

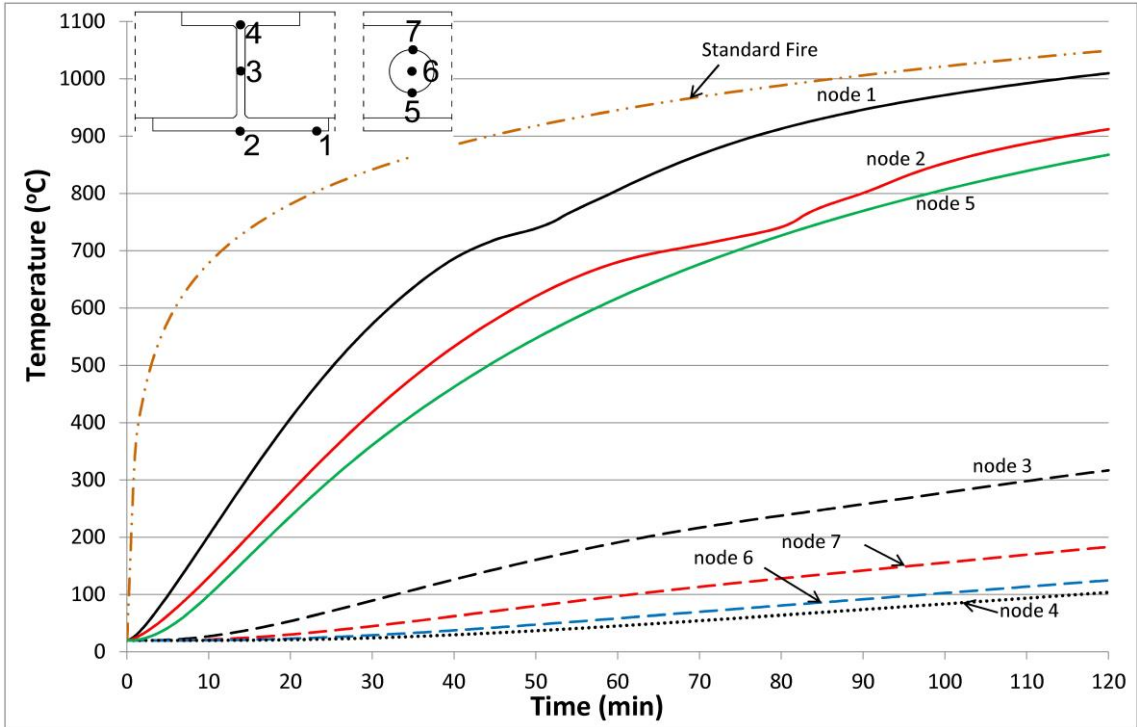


350
351

352
353 (c)



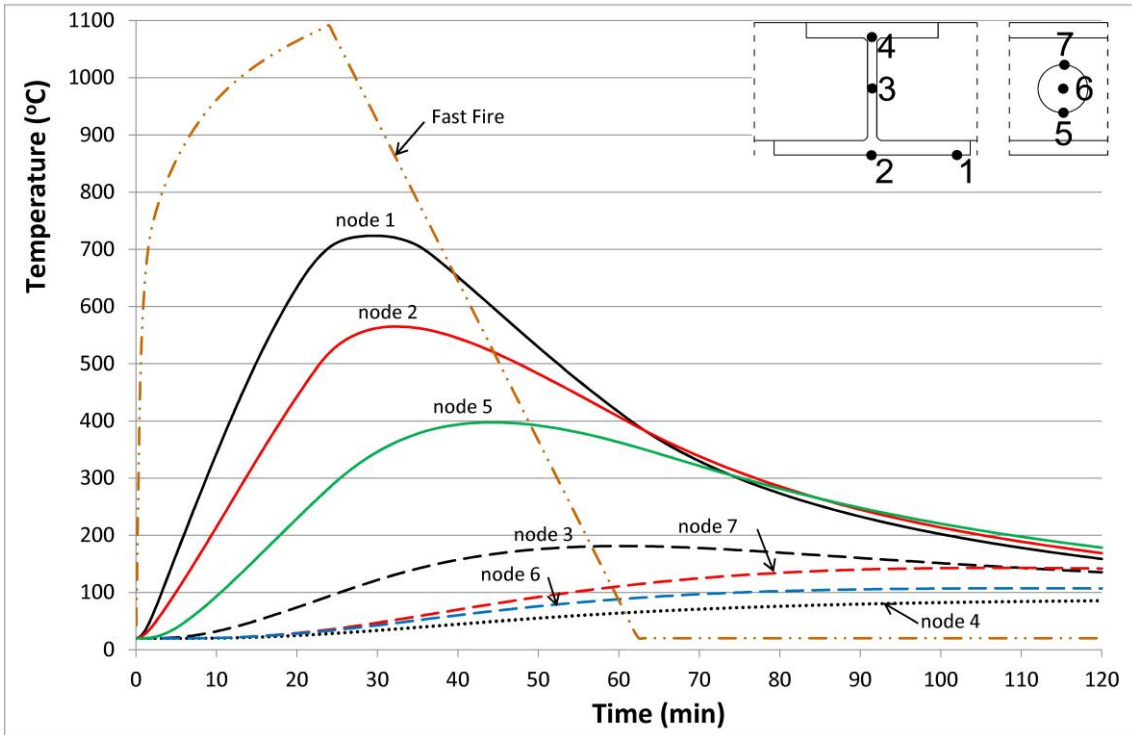
354
355 (d)



356
357

358
359

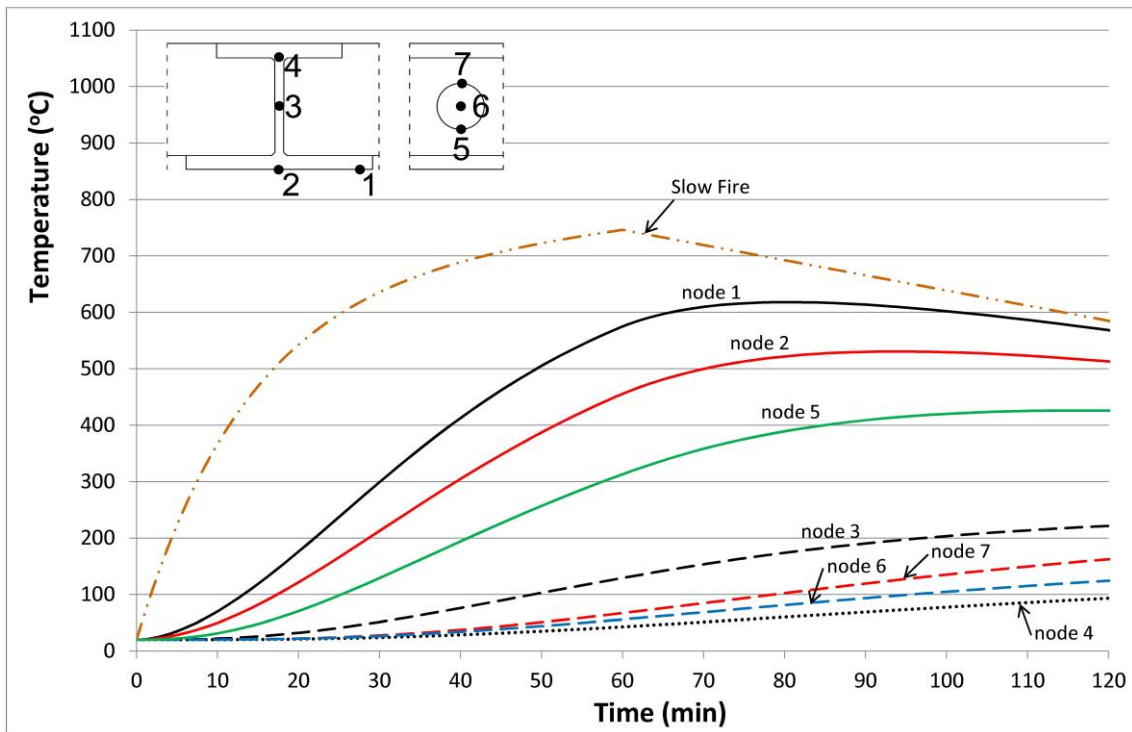
(e)



360

361

(f)



362

363

364

365

366

Figure 7. Temperature vs time relationships for unprotected Beam A and (a) standard fire, (b) fast fire, (c) slow fire exposure and for unprotected Beam B and (d) standard fire, (e) fast fire, (f) slow fire exposure.

367
368
369
370

Table 2 Developed temperatures for different fire exposures for the maximum developed temperature at node 1 with slow fire exposure ($\theta=650\text{ }^{\circ}\text{C}$) for Beam A.

Fire Exposure Node No According Figure 7	Slow Fire $t = 73.07\text{ min}$	Fast fire $t = 16\text{ min}$	Standard fire $t = 29.33\text{ min}$
Node 1	650 °C	656 °C	655 °C
Node 2	578 °C	502 °C	533 °C
Node 5	460 °C	283 °C	354 °C
Node 3	252 °C	107 °C	157 °C

371
372
373
374
375

Table 3 Developed temperatures for different fire exposures for the maximum developed temperature at node 1 with fast fire exposure ($\theta=796\text{ }^{\circ}\text{C}$) for Beam A. Results for slow fire exposure are not presented, as node 1 does not reach the target temperature pf 796 °C.

Fire Exposure Node No According Figure 7	Fast fire $t = 25.95\text{ min}$	Standard fire $t = 48.33\text{ min}$
Node 1	796 °C	797 °C
Node 2	680 °C	706 °C
Node 5	433 °C	517 °C
Node 3	189 °C	256 °C

376

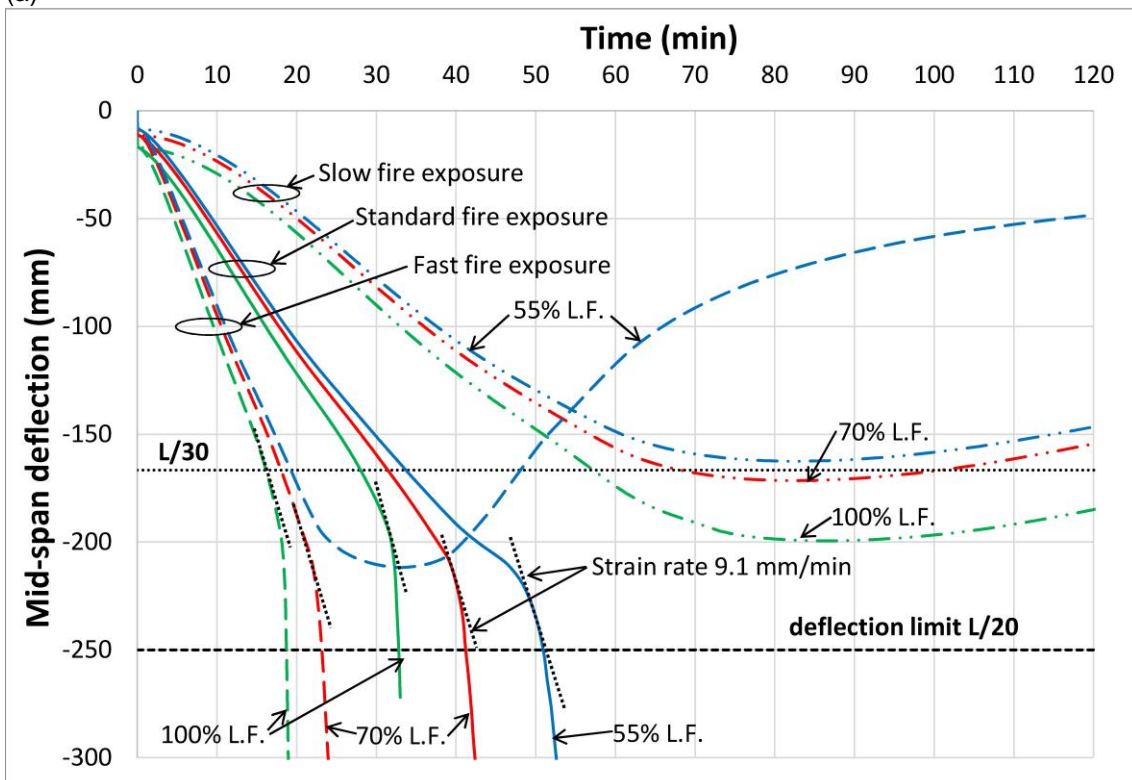
377 **4.2.2 Structural response**

378 The simulation results for the unprotected Beam A are presented in Figure 8(a). The initial
379 slopes of the mid-span deflection are affected by different thermal gradients as discussed in the
380 previous section. When Beam A is exposed to the fast fire, the fire resistance is limited to 15
381 and 20 min for load factors 100% and 70%, respectively. Under the same fire conditions, Beam

382 A survives the full duration of the fast fire when the load ratio is 55%. Beam A also survives the
 383 full duration of the slow fire for all load factors applied. The fire resistance, when exposed to the
 384 standard fire, is between 30 and 50 min depending on the applied load factor.

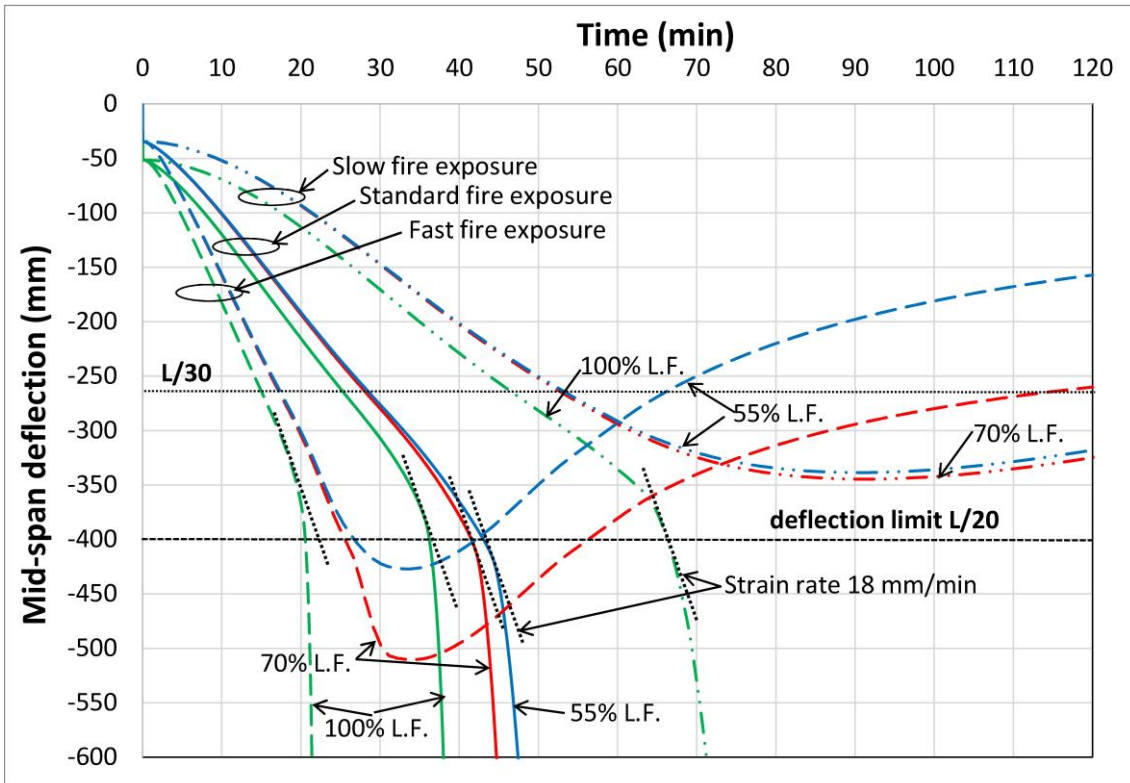
385 From the structural analysis of the unprotected Beam B presented in Figure 8(b), similar results
 386 to those for Beam A are obtained. When it is exposed to standard fire, the fire resistance is
 387 limited between 35 and 45 mins for the various load factors, despite that it has higher section
 388 factor and some over-strength in bending. When exposed to the slow parametric fire, Beam B
 389 survives the full duration of the slow fire for load factors 55% and 70%. When the load factor is
 390 100% the beam fails after 65 min of slow fire exposure. Similarly, for the fast parametric fire
 391 exposure, when the applied load factor is 100% the beam has fire resistance less than 20 min.
 392 For lower load factors than 100%, the fire resistance is approximately 20 min. The fire
 393 resistance is limited in these cases (fast fire exposure, load factors 70% and 55%) due to the
 394 excessive deformation caused by thermal gradients. As it can be seen in Figure 8(b), Beam B
 395 survives the full duration of the fast fire for these load factors, and if a performance-based
 396 approach was employed, the fire resistance could be estimated as R120 or higher.

397 (a)



398
 399

(b)



400
401
402
403
404
405

Figure 8. Mid-span deflection vs time for unprotected (a) Beam A and (b) Beam B for 55%, 70% and 100% load factors and different fire exposures (standard, fast, slow).

4.3 Performance of protected USFBs

406 In this section, the performance of protected USFBs is discussed in terms of developed
407 temperatures (thermal response) and fire resistance (structural response) for three different
408 intumescent coating thicknesses (0.4, 0.8, 1.2 mm).

409

4.3.1 Thermal response

411 The temperatures against time relationships are presented in Figure 9. Figure 9 (a) to (c)
412 presents the thermal analysis results for Beam A while Figure 9 (d) to (f) represent Beam B for
413 different fire exposure curves.

414 Beam A under standard fire exposure develops high average temperatures at the bottom flange
415 (average temperature of node 1 and 2, Figure 9(a)). After 60 minutes of standard fire exposure,
416 the average bottom flange temperatures are 640 °C, 510 °C and, 465 °C for 0.4 mm, 0.8 mm
417 and 1.2 mm thickness of applied intumescent coating, respectively, in comparison with the
418 unprotected beam developed maximum temperature of 775 °C. After 90 minutes of standard fire
419 exposure, the average bottom flange temperatures are 700 °C, 605 °C and, 565 °C for 0.4 mm,

420 0.8 mm and 1.2 mm thickness of applied intumescent coating, respectively. After 90 minutes of
421 standard fire exposure the unprotected beam had average bottom flange temperature 895 °C
422 (Figure 9 (d)). Similarly, Beam B, after 60 min of standard fire exposure had average bottom
423 flange temperature 555 °C when protected with 0.4 mm of intumescent coating, instead of 740
424 °C when unprotected. After 90 minutes of standard fire exposure, the average bottom flange
425 temperature was 630 °C for 0.4 mm protection, while the unprotected beam developed 860 °C.
426 The temperatures at nodes 3 and 4 are mostly lower than 400 °C and so they are not important.
427 When exposed to fast parametric fire, Beam A at node 1 develops maximum temperature 630
428 °C (Figure 9 (b)) when protected with 0.4 mm protection. The average bottom flange
429 temperature is 550 °C. For 0.8 mm thickness of intumescent coating the maximum average
430 temperature of the bottom flange is 465 °C. Similarly, Beam B develops maximum average
431 bottom flange temperatures 485 °C and 360 °C for 0.4 and 0.8 mm thickness of intumescent
432 coating. Nodes 3 and 4 develop temperatures always lower than 250 °C and so they do not
433 affect the capacity of the beam.

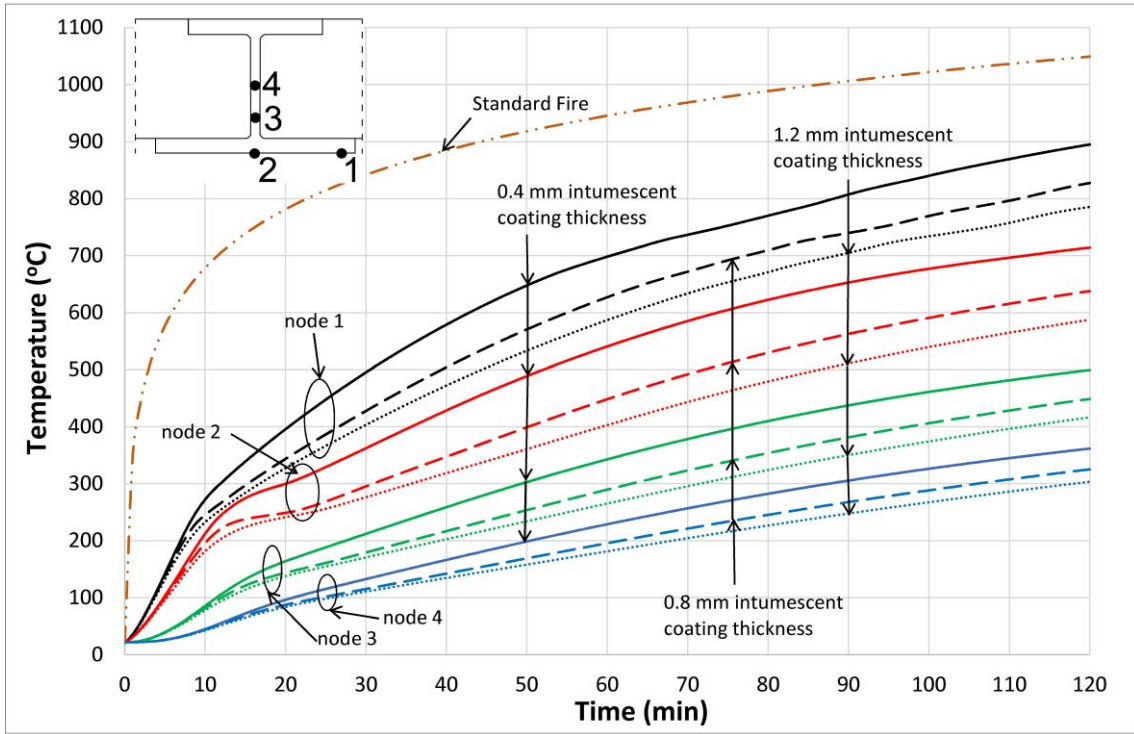
434 When Beam A is exposed to slow parametric fire (Figure 9(c)), the maximum developed
435 temperature is 500 °C and the maximum average temperature of the bottom flange is just 450
436 °C when 0.4 mm of intumescent coating is applied. For higher thicknesses of coating, and also
437 at nodes 3 and 4 the temperatures remain low. Similarly, Beam B (Figure 9(f)), under the same
438 conditions develops just 370 °C maximum average bottom flange temperature for 0.4 mm of
439 protection.

440 Typical temperature distributions are shown in Tables 4, 5, and 6 for standard, fast and low fire
441 exposure respectively. Furthermore, in these tables, the effect of insulation on the temperature
442 distribution of the cross-section is shown.

443

444
445

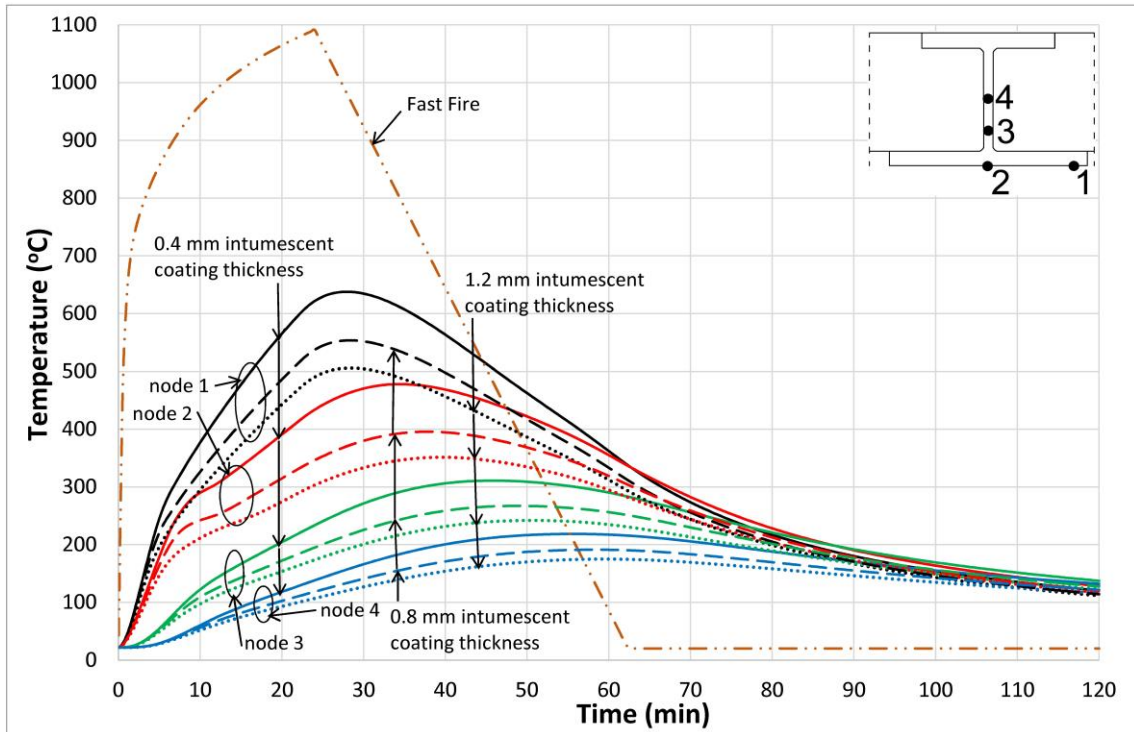
(a)



446

447

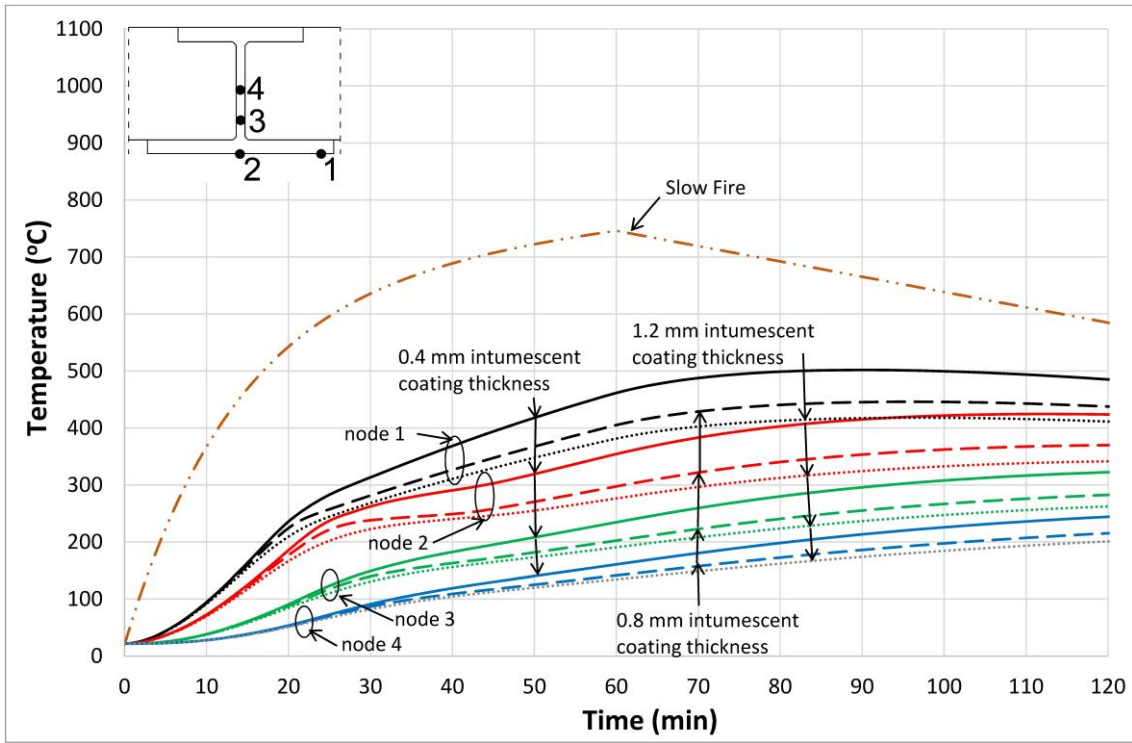
(b)



448

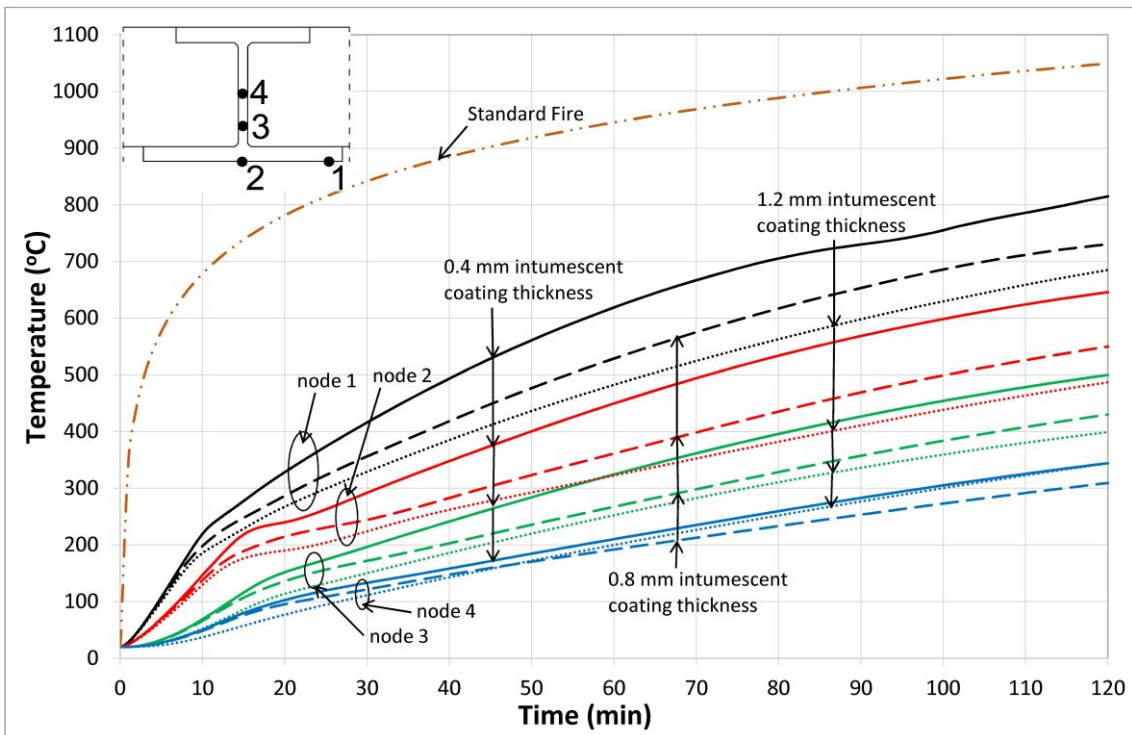
449

450
451 (c)



452

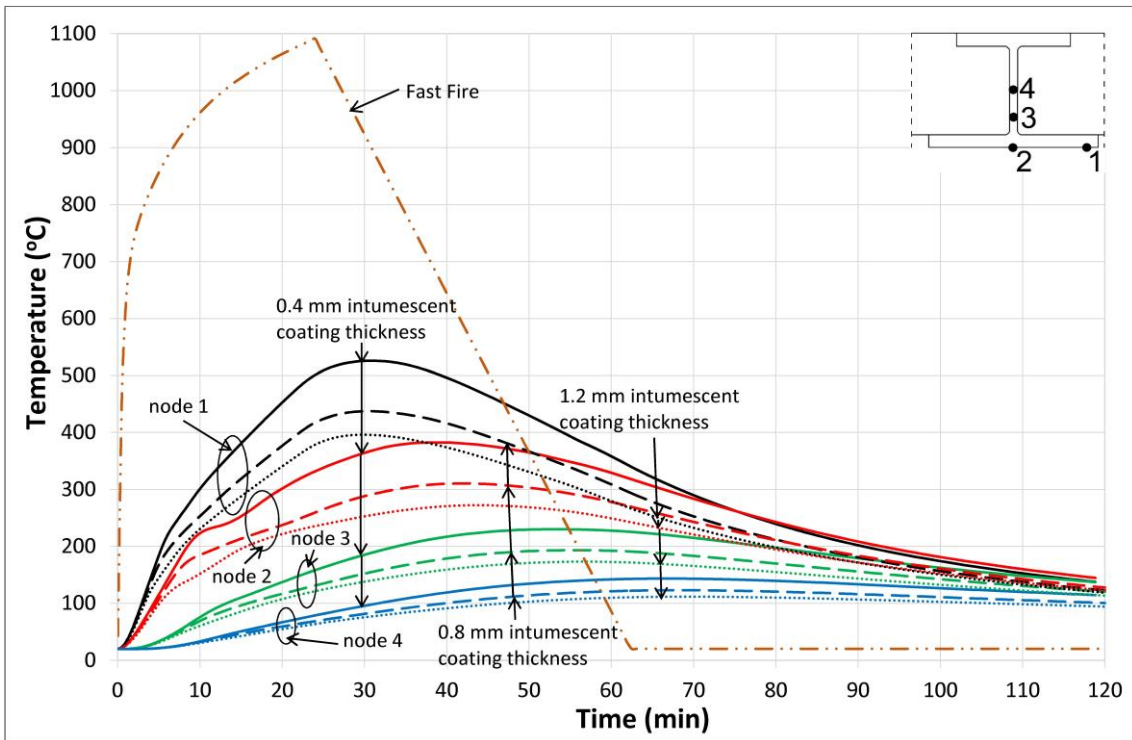
453 (d)



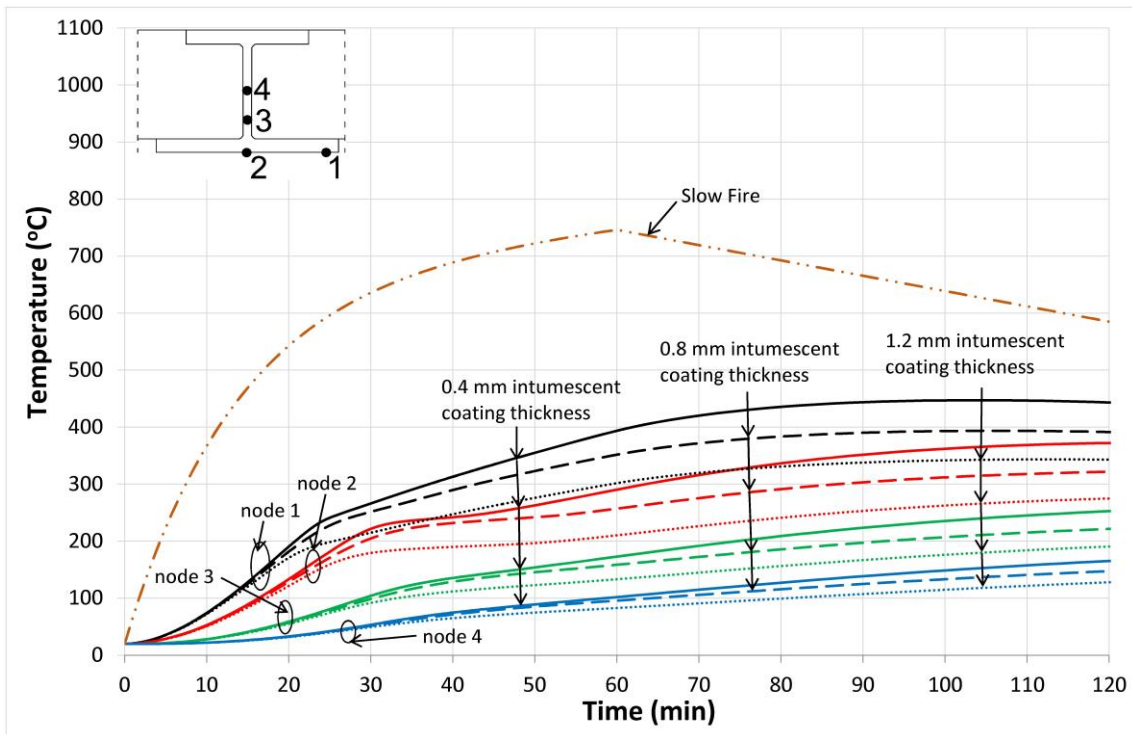
454

455

456
457 (e)



458
459 (f)



460

461 **Figure 9.** Temperature vs time relationships for Beam A and (a) standard fire, (b) fast fire, (c)
462 slow fire exposure and for Beam B and (d) standard fire, (e) fast fire, (f) slow fire exposure,
463 protected with 0.4, 0.8, and 1.2 mm thickness of intumescent coating.
464

465 **Table 4** Comparison of temperature development of Beam A after 90 min of standard fire
 466 exposure

Node No	temperature (°C)	Ratio θ_i / θ_1	temperature (°C)	Ratio θ_i / θ_1	temperature (°C)	Ratio θ_i / θ_1	temperature (°C)	Ratio θ_i / θ_1
According to Figure 9	unprotected	unprotected	Protected 0.4 mm	Protected 0.4 mm	Protected 0.8 mm	Protected 0.8 mm	Protected 1.2 mm	Protected 1.2 mm
1	967.46	1	808.14	1	739.85	1	705.56	1
2	898.71	0.929	653.07	0.81	562.76	0.76	511.60	0.72
3	570.50	0.59	437.85	0.54	381.45	0.52	350.78	0.50
4	387.93	0.40	305.67	0.38	267.79	0.36	248.02	0.35

467

468 **Table 5** Temperature development in Beam A when temperature is maximum at node 1 for fast
 469 fire exposure

Node No	temperature (°C)	Ratio θ_i / θ_1	temperature (°C)	Ratio θ_i / θ_1	temperature (°C)	Ratio θ_i / θ_1	temperature (°C)	Ratio θ_i / θ_1
According to Figure 9	unprotected t=25.91 min	unprotected	Protected 0.4 mm t=27.95 min	Protected 0.4 mm	Protected 0.8 mm t=28.41 min	Protected 0.8 mm	Protected 1.2 mm t=28.24 min	Protected 1.2 mm
1	795.82	1	637.60	1	553.48	1	505.55	1
2	680.44	0.86	461.19	0.72	372.65	0.67	325.60	0.64
3	338.34	0.43	259.58	0.41	217.81	0.39	193.08	0.38
4	189.03	0.24	156.69	0.25	135.03	0.24	121.06	0.24

470

471 **Table 6** Temperature development in Beam A when temperature is maximum at node 1 for slow
 472 fire exposure

Node No	temperature (°C)	Ratio θ_i / θ_1	temperature (°C)	Ratio θ_i / θ_1	temperature (°C)	Ratio θ_i / θ_1	temperature (°C)	Ratio θ_i / θ_1
According to Figure 9	unprotected t=71.06 min	unprotected	Protected 0.4 mm t=91.11 min	Protected 0.4 mm	Protected 0.8 mm t=96.39 min	Protected 0.8 mm	Protected 1.2 mm t=97.06 min	Protected 1.2 mm
1	650.88	1	501.86	1	446.06	1	418.19	1
2	576.05	0.89	416.22	0.83	359.47	0.80	330.77	0.79

3	369.59	0.57	297.46	0.59	262.94	0.59	244.47	0.58
4	246.59	0.38	214.88	0.42	193.60	0.43	181.50	0.43

473

474 **4.3.2 Structural Response**

475 The structural response of beams A and B for different fire conditions and load factors in terms
 476 of fire resistance as defined in BS476-Part 20 (1987) [19] is presented in Figure 10.

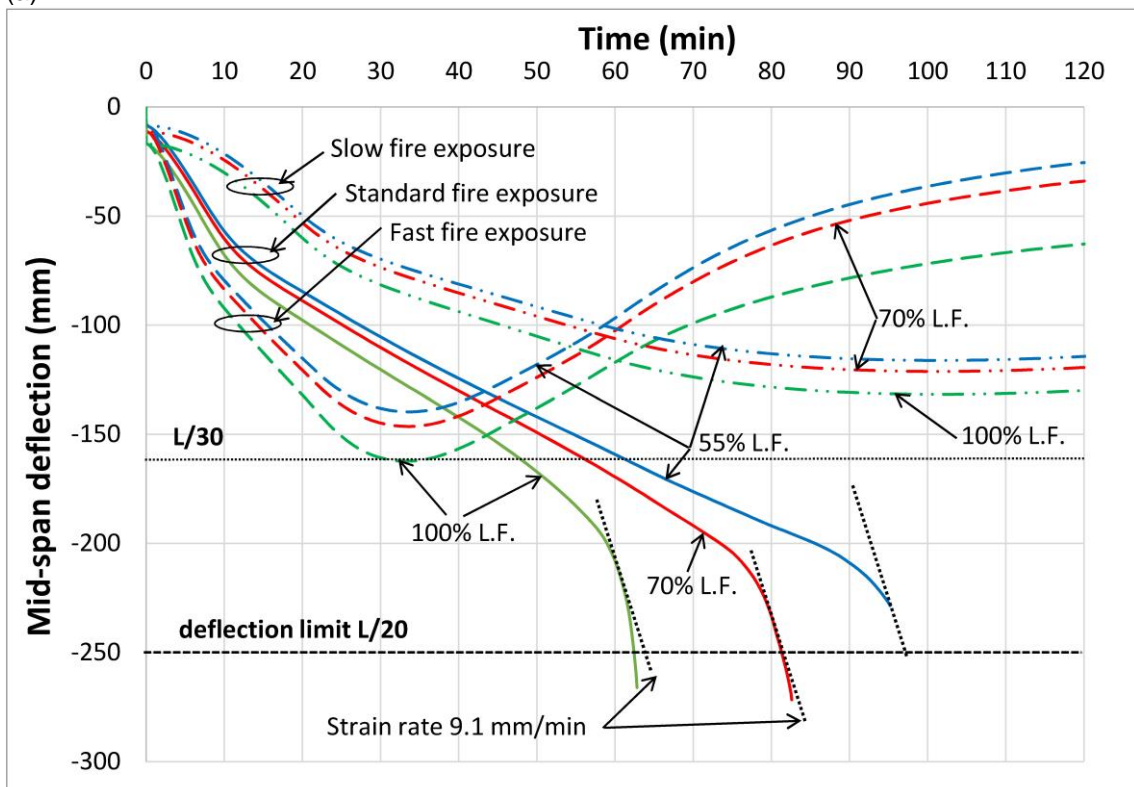
477 Both beams survive the parametric fires even when protected with the minimum of 0.4 mm of
 478 intumescent coating, for all examined load factors. During cooling phase, the bottom flange
 479 temperatures are reduced, so the bowing effect is reduced and gradually the beam is returning
 480 to its initial shape, eg the deflection due to temperature is disappearing.

481 The fire resistance of both beams under standard fire exposure is presented in Table 7.

482

483

(a)

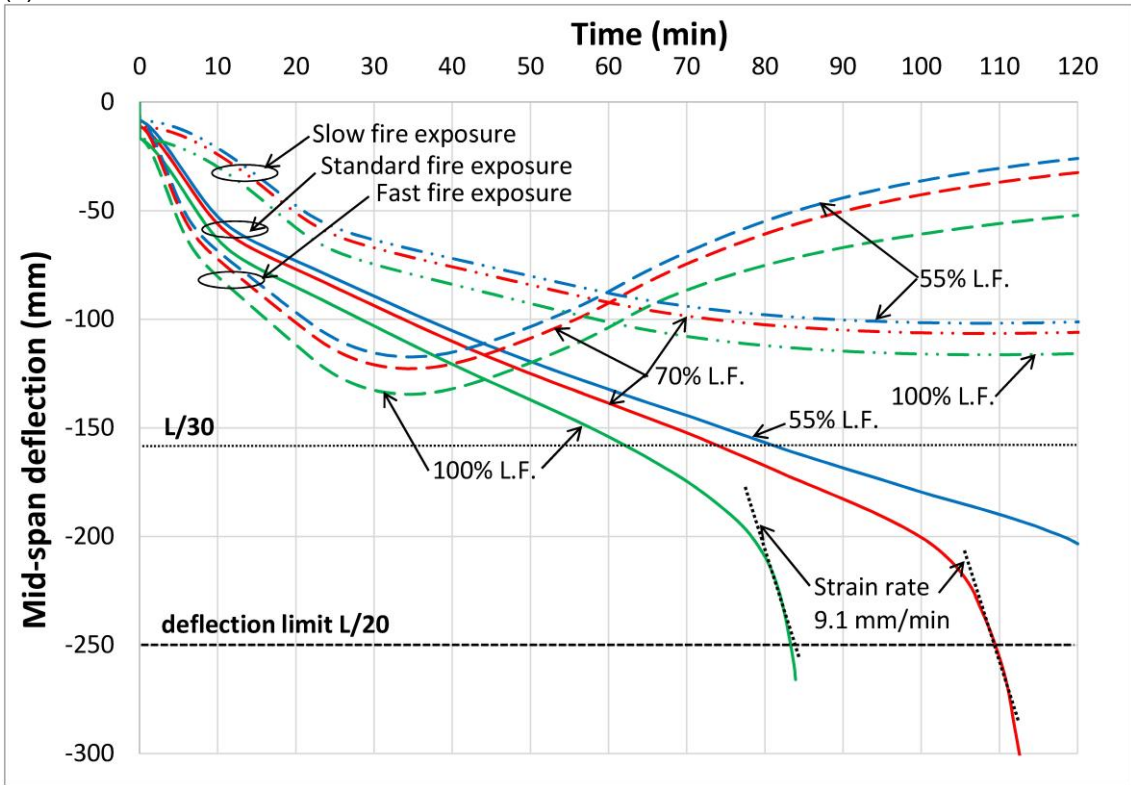


484

485

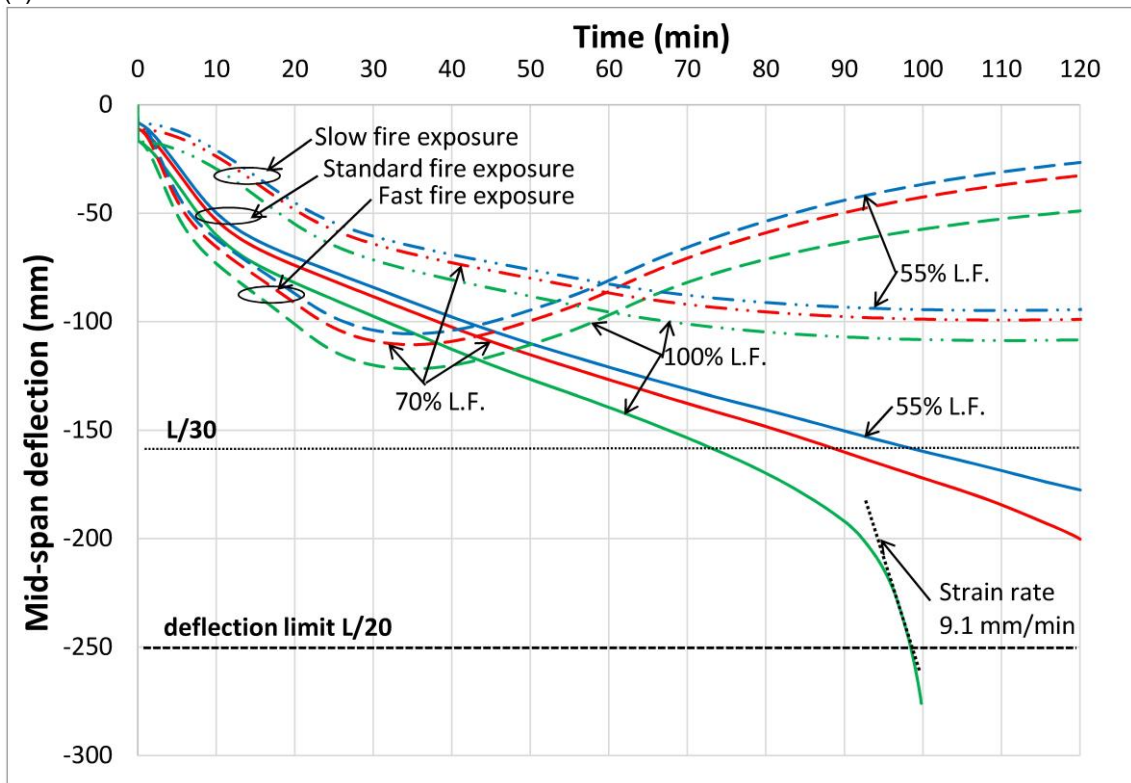
486
487

(b)



488
489

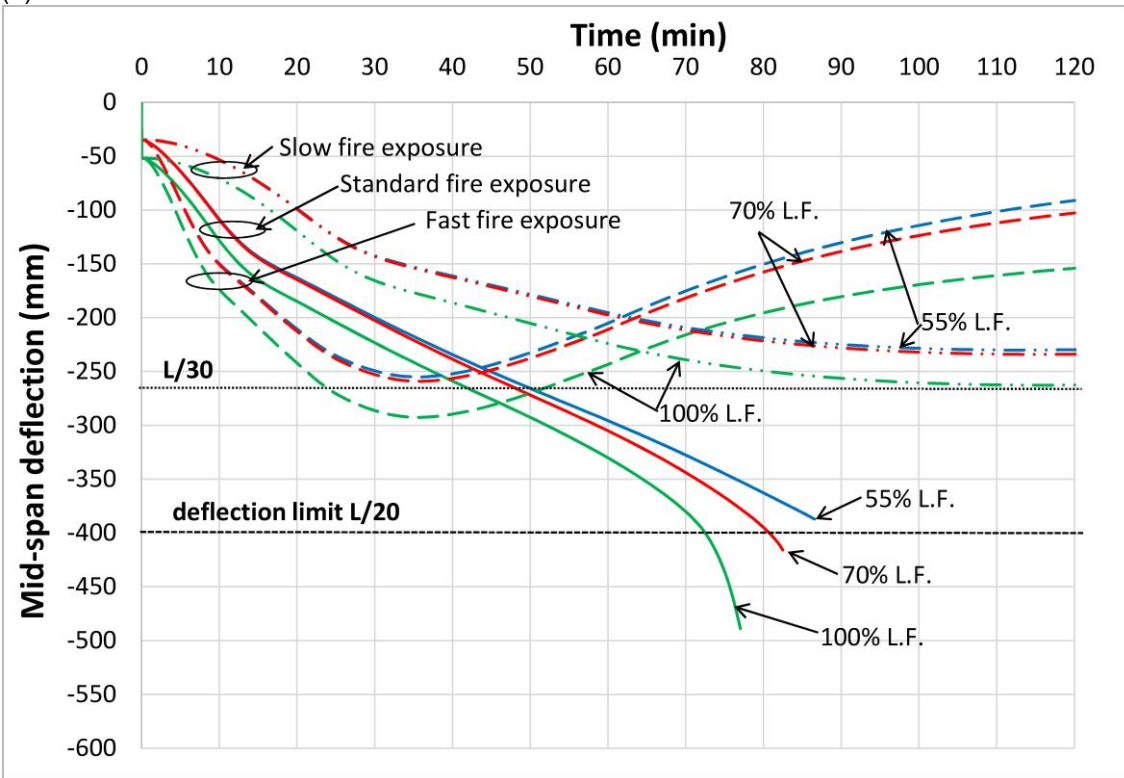
(c)



490
491

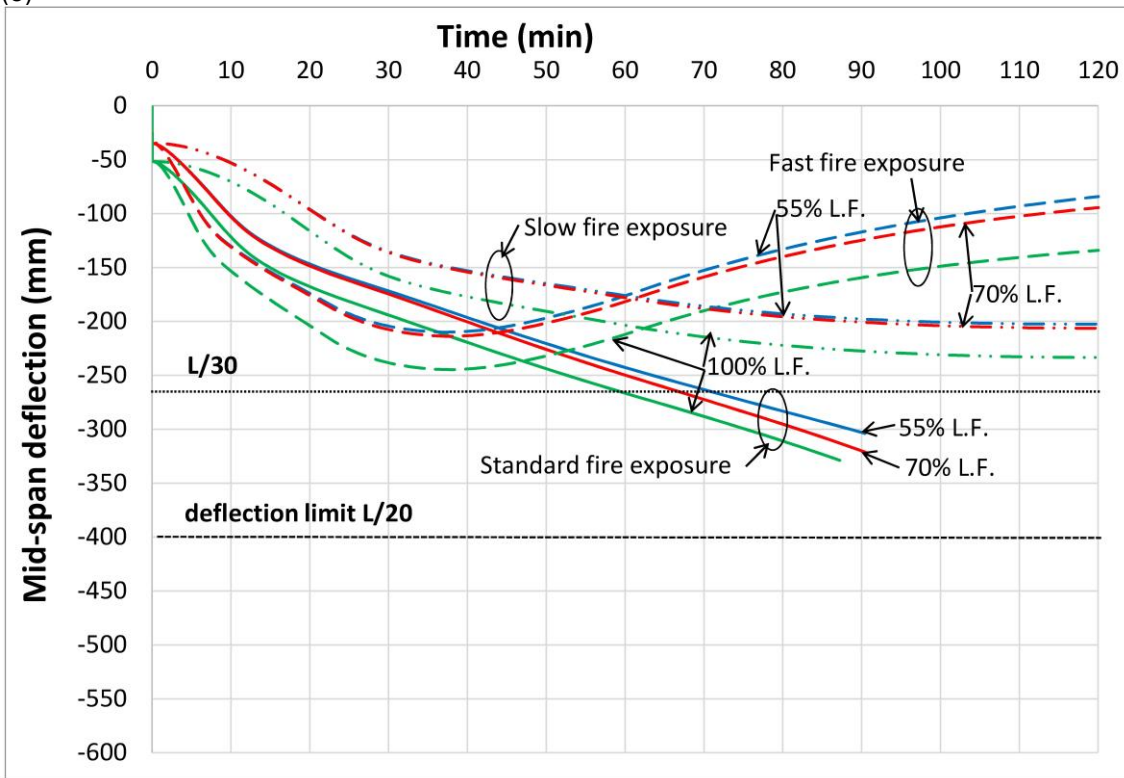
492
493

(d)



494
495

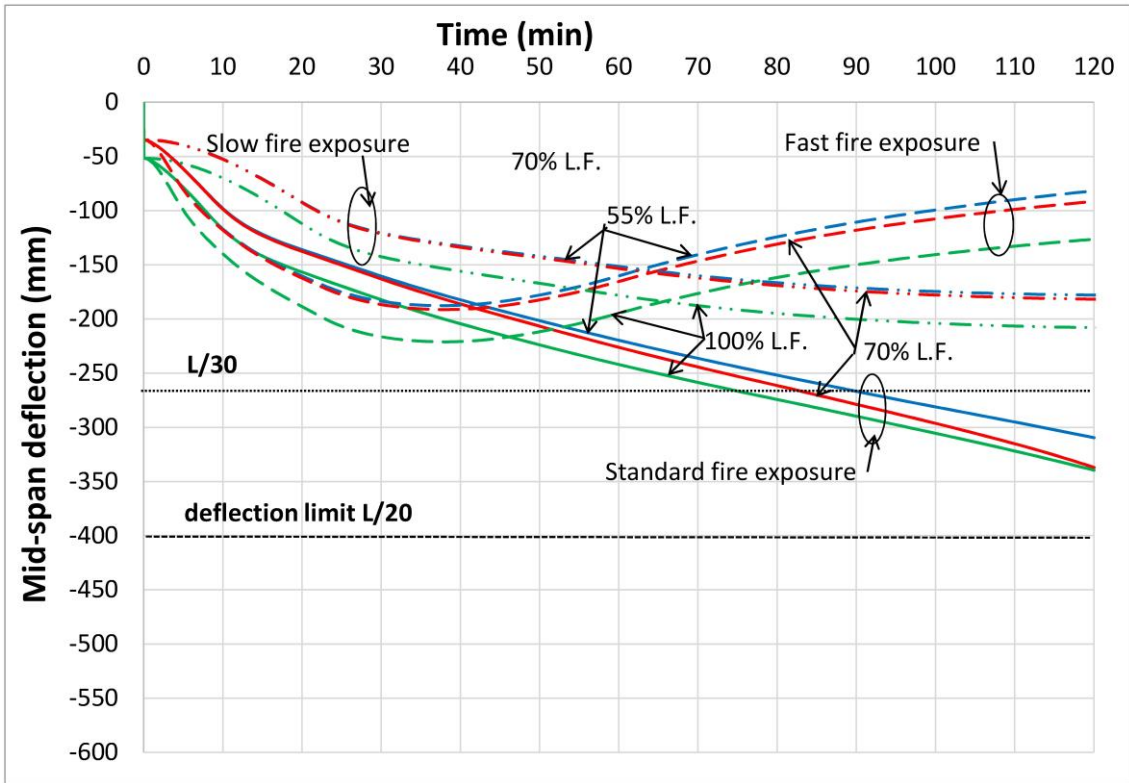
(e)



496
497

498
499

(f)



500
501
502
503
504
505
506

Figure 10. Mid-span deflection vs time for Beam A protected with (a) 0.4 mm, (b) 0.8 mm, (c) 1.2 mm thickness of intumescent coating and Beam B protected with (d) 0.4 mm, (e) 0.8 mm, (f) 1.2 mm thickness of intumescent coating for 55%, 70% and 100% load factors and different fire exposures (standard, fast, slow).

507
508
509

Table 7. Fire resistance of protected beams A and B under standard fire exposure for different intumescent coating thicknesses and different load factors.

Thickness of intumescent coating (mm)	Fire Resistance (min)					
	Beam A			Beam B		
	Load factor			Load factor		
	100%	70%	55%	100%	70%	55%
0.4	60	80	90	60	70	80
0.8	80	100	120	80	90	100
1.2	90	120	120	120	120	120

510

511 **5. Discussion**

512 The critical temperature according EN 1994-1-2 (2005), for beam A is 385 °C and for beam B
513 460 °C as calculated in Maraveas et al (2015)[6], defined as average bottom flange
514 temperature. As it is seen in Figures 7-10, these critical temperatures are very conservative. For

515 example, unprotected beam A survives the slow fire, with average bottom flange temperature
516 575 °C even for the non-realistic load factor of 100% (Figure 7(c) and Figure 8(a)). The same
517 unprotected beam fails after approximately 35 min exposure to the standard fire and when the
518 average bottom flange temperature is approximately 600 °C (Figure 7(a) and Figure 8(a)). The
519 difference, in terms of critical temperatures, between EN 1994-1-2 (2005) [7] and the FEM
520 results is relevant to the stress redistribution when the bottom flange is very hot and the
521 contribution of the concrete slab. Most flooring systems with partially protected cross-section in
522 fire experience similar performance [21]. The bottom flange temperatures are function of the
523 cross-section factor, eg of the exposed flange section factor. Thicker flanges will develop lower
524 temperatures and will have improved performance in fire. Similarly, the thickness of the steel
525 web also has a role in fire resistance of the USFBs. A USFB with thicker web, especially the
526 bottom half, give a better fire resistance. Further, the depth of the USFBs may dictate their fire
527 resistance as the thermal gradient plays a vital role in their fire performance. For deeper USFBs,
528 the thermal gradient may be higher and for shallower USFBs, the thermal gradient may be
529 lower. For similar thicknesses of the flanges and steel web, a USFB with larger depth may
530 provide a higher fire resistance as compared to a USFB with a smaller overall depth.
531 When the beams are exposed to parametric fires, they survive with just a minimum of
532 protection. This leads to low cost solution, compatible with the predictions of Eurocodes and in
533 parametric fire exposures. Parametric fires are realistic, on the contrary, the standard fire is non-
534 realistic and it is used for historical reasons.

535 This research is limited to simply supported beams. More complex structural systems need
536 further research and the conclusions of this research may not applied.

537

538 **6. Concluding remarks**

539 The paper presents a numerical investigation on the performance of Ultra Shallow Floor Beams
540 exposed to standard and parametric fires. Two different simply supported USFBs with different
541 span lengths and cross-sections have been examined under different fire exposure conditions
542 and load factors. Both unprotected and protected beams were considered with intumescent
543 coating of three different thicknesses. From the FEM results, the following conclusions can be
544 drawn:

- 545 - Although it is a common practice to apply the fire protection materials on the bottom
546 exposed steel flange of the USFBs, it was found that USFBs can survive slow
547 parametric fires under realistic load factors without the fire protection materials. This will
548 help with reducing the cost of structures without comprising their fire resistance. The
549 reduction in the application of fire protection materials should always be based on the
550 results of performance-based design. For example, during this study, it was found that
551 with a layer of 0.4 mm intumescent coating the USFBs can survive a full duration of a
552 compartment (fast or slow) fire.
- 553 - Like other structural members, the increase in thickness of the fire protection material
554 helps in achieving a higher fire resistance of USFBs. During this study, the minimum
555 thickness of the applied intumescent coating as fire protection material was 0.4 mm. It
556 was found that the USFBs can survive both fast and slow parametric fire exposures
557 under any realistic load factor when protected with 0.4 mm thickness of intumescent
558 coating. This thickness of the applied fire protection material is significantly lesser than
559 the current practice used during construction. Further research is required for cross-
560 sections with different section factors.
- 561 - It was found that the fire resistance of USFBs is sensitive to the applied load factor as
562 well as to the type of fire exposure irrespective of the level of the applied fire protection.
563 USFBs with a lesser thickness of the fire protection materials underwent larger
564 deflections as compared to the USFBs with higher thickness of the fire protection under
565 similar applied loads.
- 566 - Although the USFBs offer a good fire resistance with little or no fire protection when
567 exposed to fast and slow parametric fires respectively, their response in standard fires
568 is more demanding. USFBs can only reach high levels of fire resistance (like R90 and
569 R120) when exposed to standard fires only with the aid of a thick intumescent coating
570 or combination of intumescent coating and low load ratio.
- 571 - The fire design approach proposed for composite beams in EN1994-1-2 (2005) is more
572 suitable for steel-concrete beams with hanging steel beam sections. These design
573 approaches when applied to USFBs produce safe but highly conservative and
574 uneconomical results. The outcomes of this study have shown that the current fire

575 design recommendations given in EN1994-1-2 (2005) needs to be modified. There is a
576 need to develop similar fire design approaches which are less conservative and more
577 suited to USFBs.

578

579 **Acknowledgements**

580 The authors would like to thank Professor Yong C. Wang, School of Mechanical, Aerospace and
581 Civil Engineering, University of Manchester, for his guidance relate to the thermal conductivity
582 and other properties of intumescent coatings.

583

584

585

586

587 **References**

- 588 1. Ahmed, I.M., Tsavdaridis K.D. (2019), The evolution of composite flooring systems:
589 applications, testing, modelling and eurocode design approaches, *Constructional Steel*
590 *Research*, 155, pp 286-300.
- 591 2. Tsavdaridis, K.D., D'Mello, C. and Huo, B.Y. (2009). Computational study modelling the
592 experimental work conducted on the shear capacity of perforated concrete-steel Ultra
593 Shallow Floor Beams (USFB). In *Proceedings of 16th Hellenic Concrete Conference* (p.
594 159).
- 595 3. Huo B. Y. and D'Mello C. A. (2013), Push-out tests and analytical study of shear transfer
596 mechanisms in composite shallow cellular floor beams, *Constr. Steel Res.*, vol. 88, pp. 191–
597 205.
- 598 4. Tsavdaridis K. D., D'Mello C., and Huo B. Y. (2013), “Experimental and computational study
599 of the vertical shear behaviour of partially encased perforated steel beams,” *Eng. Struct.*,
600 vol. 56, no. January, pp. 805–822.
- 601 5. Kansinalli, R. and Tsavdaridis, K.D. *Vibration Response of USFB Composite Floors*. The
602 13th Nordic Steel Construction Conference (NSCC 2015). 23-25 September, 2015,
603 Tampere, Finland.
- 604 6. Maraveas C., Tsavdaridis K. D. and Nadjai A. (2015), Fire resistance of unprotected Ultra
605 Shallow Floor Beams (USFB) A numerical investigation, *Fire Technol.*, 53, pp 609-627.
- 606 7. EN 1994-1-2: (2014). Eurocode 4, part 1-2: Design of composite steel and concrete
607 structures - General rules — Structural fire design. European Committee for
608 Standardization.
- 609 8. Alam, N., Nadjai, A., Maraveas, C., Tsavdaridis, K.D. and Ali, F. (2018) Response of
610 Asymmetric Slim Floor Beams in Parametric Fires. *Journal of Physics: Conference Series*,
611 1107, 032009
- 612 9. Maraveas, C., Wang, Y.C., Swales, T. (2017), Reliability based determination of material
613 safety factor for cast iron beams in jack arched construction exposed to standard and
614 natural fires, *Fire Safety Journal*, 90, pp 44-53.

- 615 10. Maraveas, C., Swailes, T. & Wang, Y., (2012). A detailed methodology for the finite element
616 analysis of asymmetric slim floor beams in fire. *Steel Construction*, 5 (3), pp 191-198.
- 617 11. Tsavdaridis, K.D., D'Mello, C. and Hawes, M. Experimental Study of Ultra Shallow Floor
618 Beams (USFB) with Perforated Steel Sections. The 11th Nordic Steel Construction
619 Conference 2009 (NSCC 2009). 2-4 September 2009, Malmö, Sweden, Reference no: 128,
620 pp. 312-319.
- 621 12. de Silva D., Bilotta A., Nigro E. (2019). Experimental investigation on steel elements
622 protected with intumescent coating. *Constr Build Mater*, 205, pp. 232-244
- 623 13. Cirpici B.K., Wang Y.C., Rogers B. (2016). Assessment of the thermal conductivity of
624 intumescent coatings in fire. *Fire Safety Journal*. 81, pp 74-84
- 625 14. Dai X., Wang Y.C. and Bailey C. (2010). A Simple Method to Predict Temperatures in Steel
626 Joints with Partial Intumescent Coating Fire Protection. *Fire Technology*, 46. pp 19–35
- 627 15. EN1991-1-2 (2009), Eurocode 1 – Actions on structures – Part 1–2: General Rules –
628 Structural Fire Design, European Committee for Standardization.
- 629 16. Alam, N., Nadjai, A., Ali, F., & Nadjai, W. (2018). Structural response of unprotected and
630 protected slim floors in fire. *Constructional Steel Research*, 142, pp.44–54.
- 631 17. Bourbigot S., Le Bras M., Delobel R. (1995). Fire Degradation of an Intumescent Flame
632 Retardant Polypropylene using the Cone Calorimeter. *Journal of Fire Sciences*.
633 <https://doi.org/10.1177/073490419501300101>
- 634 18. Bailey, C.G., (1999). The behaviour of asymmetric slim floor steel beams in fire. *Journal of*
635 *Constructional Steel Research*, 50(3), pp.235–257.
- 636 19. BS 476 Part-20 (1987). Fire tests on building materials and structures. Method for
637 determination of the fire resistance of elements of construction
- 638 20. ISO 834–1 (1999) Fire-resistance tests—elements of building construction—part 1: general
639 requirements. ISO, Switzerland.
- 640 21. SCI (2008) Steel Construction Institute, Slimflor compendium, Document RT1147
641